Chapter 18
Hybrids with Functional Dyes

Juraj Bujdák

Abbreviations

$^1\Delta_g$	Singlet oxygen
CEC	Cation exchange capacity
ED	Energy donor
EA	Energy acceptor
FRET	Förster resonance energy transfer
Hec	Hectorite
Lap	Laponite
LB	Langmuir–Blodgett
LbL	Layer-by-layer
LDH	Layered double hydroxide(s)
LNb	Layered niobate(s)
LSil	Layered silicate(s)
LTi	Layered titanate(s)
MB	Methylene blue
Mmt	Montmorillonite(s)
NLO	Nonlinear optical (or nonlinear optics)
RCMs	Reduced-charge montmorillonites
Rh	Rhodamine
ROS	Reactive oxygen species
Sap	Saponite
UV	Ultraviolet

J. Bujdák (✉)
Faculty of Natural Sciences, Department of Physical and Theoretical Chemistry, Comenius University in Bratislava, 842 15 Bratislava, Slovakia
e-mail: bujdak@fns.uniba.sk

J. Bujdák
Institute of Inorganic Chemistry, Slovak Academy of Sciences, Bratislava, Slovakia

T. Nakato et al. (eds.), *Inorganic Nanosheets and Nanosheet-Based Materials*, Nanostructure Science and Technology, DOI 10.1007/978-4-431-56496-6_18

18.1 Introduction

Hybrid materials are composed of at least two constituents and structurally built at the nanometer or molecular scale. The constituents may include molecules, functional groups, molecular fragments, polymeric chains, nanosheets, nanotubes, or other types of nanoparticles. Hybrid materials often exhibit multifunctional properties and have potential for various applications. Hybrids with organic dyes adsorbed on the surface of nanosheets or embedded in the crystals of layered compounds involve a very broad range of material types with variable structures, functionalities, and properties. Probably, the oldest hybrid material of this type is Maya blue, the pigment used by the Maya and Aztec civilizations in the era of pre-Columbian America. Maya blue is composed from indigo dye from the plant *Indigofera suffruticosa* intercalated in a clay mineral, palygorskite. The host particles of palygorskite do not contribute to the color of the pigment, but play an active role in the chemical stabilization of the dye. It is remarkable how long Maya blue paintings have lasted, despite the paints being exposed to harsh climatic conditions, high temperature and humidity. The properties of Maya blue inspired scientists, who tried to mimic its nature by developing similar types of materials [1–3]. In the modern era, the paint industry was probably one of the first branches to develop pigments based on composites of inorganic compounds with organic dyes. Inorganic solids were often used as the carriers of dye molecules, fillers, or pigment additives. Hybrid materials and nanomaterials incorporating organic dyes have only been extensively developed over the last few decades. In numerous cases, nanosheets and layered nanoparticles exhibit important functionalities and contribute to the materials' photophysical and photochemical properties. Examples include graphene and related compounds, layered semiconductors (metal oxides, hydroxides, sulfides), luminescent rare earth metal hydroxides, layered perovskites, etc. This chapter focuses on hybrid materials based on organic dyes representing the key components in terms of the materials' functionality. The dyes play primary roles in terms of the materials' optical and photofunctional properties. The inorganic components play mostly a passive role. On the other hand, inorganic layered compounds are able to significantly affect the properties of dye molecules. The inorganic layered compounds primarily include layered silicates (LSil), layered double hydroxides (LDH), but also other types. Hybrid materials with active organic dyes have been the focus of a lot of deserved attention for a few decades now. One of the first breakthrough review articles dealing with the photochemistry of such materials was published about 20 years ago [4]. This review was an inspiration for many researchers, providing original and critical perspectives on various aspects of materials of this type. Since then, thousands of papers, dozens of reviews [5–15] and several monographs and chapters [16–18] analyzing current knowledge of the topic have been published. This chapter emphasizes the

importance of the inorganic constituents in the properties of adsorbed or embedded organic dye molecules, analyzing primarily the latest knowledge published over the last decade. This chapter also explains the principles of the routes for the synthesis of active hybrid material and summarizes the phenomena occurring in these hybrid systems. Last but not least, it highlights the current state and promise of potential applications.

18.1.1 Basic Features of the Hybrids with Photoactive Dyes

Hybrids with photoactive nanosheets have received a lot of attention. However, using inert layered substrates can be advantageous in many cases. The photoactive inorganic compounds can initialize the photodecomposition of organic dyes. For example, layered titanates (LTi) are more efficient photocatalysts than standard commercial materials based on TiO_2 [19]. Some organic dyes are efficiently protected by the inert particles of LSil, whereas they decompose in the presence of photoactive layered niobates (LNb) [20]. Even mixtures of active and nonactive layered nanoparticles can significantly improve the protection of dye molecules compared to the pure semiconductor colloids. Examples are mixtures of exfoliated particles of LNb or LTi with LSil [21, 22].

The parameters of both the dyes and nanoparticle components are important to successfully design hybrid materials. The most important parameters of dye molecules include their molecular geometry and shape, charge and the distribution of functional and ionic groups, and hydrophobic or hydrophilic properties. The parameters of nanoparticles are more complex, depending on the type of layered compound, particle structure, surface reactivity, and topography. The presence of particle surface charge creates an electrostatic field affecting the orientation of polar molecules and controls the arrangement and distribution of charged ions. Ion exchange reactions have been traditionally used for the synthesis of hybrid materials of LSil and LDH. Organic counterions are irreversibly adsorbed onto the surface of nanoparticles. The binding coefficients of cationic organic dyes on the surface of LSil are several orders of magnitude larger than those of inorganic cations [23]. The dye adsorption often exceeds the cation exchange capacity (*CEC*). Molecular orientation depends on the degree of dye loading, on the size and molecular shape of dye molecules, and the presence of ionic groups. Anisotropy is one of the most important properties which can be implemented for anisotropic materials applicable in optical devices. Interesting properties can be expected based on the specific host–guest interactions leading to significant changes in dye properties. This might result from dye molecular aggregation, or can relate to the changes in dye geometry or electronic properties. Photophysical phenomena occurring in hybrid systems, such as resonance energy transfer or nonlinear optical (NLO) properties increase the attractiveness of such hybrid materials.

18.2 Surface and Structural Parameters of Inorganic Nanolayered Compounds

There is a large spectrum of inorganic layered compounds which are potential sources for nanosheets or layered particles for hybrids with functional dyes. They involve graphene, LSil, LDH, hydroxides, LTi, LNb, layered oxides, vanadates, phosphates, phosphonates, sulfides, nitrides, and others. Some basic information on these compounds is available in the literature (e.g. [24–26]). A typical example of nanolayered compounds with chemically inert surfaces are expandable LSil. They include smectites, which are expandable clay minerals such as montmorillonite (Mmt), saponite (Sap), hectorite (Hec), and related synthetic materials, such as Laponite (Lap). The particles of expandable LSil are about 0.96 nm thick, with diameters ranging from several tens to several hundreds of nm, up to a few μm. The individual layered particles of LSil are built from sheets of octahedrons and tetrahedrons linked together by covalent bonds. The octahedral sheet is based mostly on Al^{III}, Fe^{III}, Fe^{II}, Mg^{II} or Li^{I} central atoms, and O^{II-}, OH^-, F^- ligands. The occupancy in the octahedral sheets positions may lead to either a dioctahedral or trioctahedral structure. Tetrahedrons are occupied by predominantly Si^{IV} and Al^{III} central atoms. One octahedral sheet is sandwiched between two covalently bound sheets of tetrahedrons to form an individual layer. Nonequivalent isomorphous substitutions and vacancies in both the octahedral or tetrahedral sheets create a net negative charge, which is balanced by mobile exchangeable cations. The layer charge controls the distribution of exchangeable cations and plays key roles in various properties of the material. In the systems with cationic dyes, charge distribution sensitively controls the molecular aggregation [12, 27, 28] (see Sect. 18.4.3) and orientation of dye cations [29, 30] (see Sect. 18.5.1). Whereas LSil nanoparticles are built from three sheets of polyhedrons, LDH or layered hydroxides are composed of single sheets of polyhedrons of individual particles (Fig. 18.1). The topography of the particle surface at the atomic level and the presence of functional groups at the surface are very important in terms of adsorption and surface activity. One example is the specific orientation of rhodamine (Rh) and oxazine dyes in LSil hybrid films, where the inclination angle of the dyes with respect to the surface depends on the type of amine groups ($–NH_2$, –NHR, $–NR_2$, where R=methyl or ethyl). The largest orientation angles were observed for dye cations with –NHR groups (60–70°) [29–33]. It is assumed that the interaction of –NHR groups carrying a positive charge is influenced by the topography of the LSil basal surface: Probably the –NHR groups specifically interact at the surface, rearranging themselves according to pseudohexagonal cavities in the surface and causing molecules to be more inclined with respect to the plane of the surface. The smaller $–NH_2$ groups give more freedom of orientation, whereas the bulkier $–NR_2$ groups do not fit into the cavities at all. There have been no systematic studies focused on dye orientation related to different topographies of variable layered compounds.

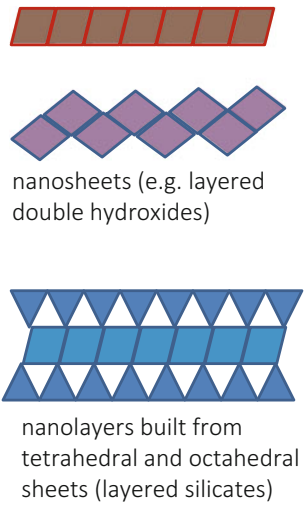

Fig. 18.1 Nanoparticles based on nanosheets or nanolayers composed from three sheets of polyhedrons

18.3 Material Types and Strategies for the Synthesis of Hybrid Materials

18.3.1 Colloids

The majority of the synthesis routes leading to hybrid materials proceeds via colloid systems with finely dispersed nanoparticles. The properties of the colloid precursors may crucially affect the quality of solid hybrid materials. The main parameter affecting the stability of colloidal systems is surface charge, which is compensated by the counterions of either an inorganic or organic type. The properties of the ions significantly affect swelling, interparticle associations, and particle exfoliation. LSil with Na^+ or Li^+ counterions swell macroscopically, forming finely dispersed individual nanoparticles [11]. Alkylammonium cations with short alkyl chains or bulky shapes are efficient swelling agents for some layered compounds with larger charge densities [20, 34]. LDH with the particles bearing a positive charge are accessible in the form with CO_3^{-2} anions, which, however, do not form stable colloids. The swelling of LDH can be achieved in organic polar solvents with NO_3^- or ClO_4^- counterions [35, 36]. However, the replacement of CO_3^{-2} anions is not easy [37, 38], and LDHs saturated with NO_3^- or ClO_4^- anions are unstable due to the presence of CO_2. The modification of LDH with organic anions of carboxylic acids, amino acids, organic sulfates can improve the stability of colloids [37]. Colloid properties are in general influenced by ionic strength, temperature, particle size, shape, and surface modification. More complex nonaqueous ternary colloidal systems sometimes including polymers or ionic surfactants have attracted a lot of attention. Premodification with large alkylammonium cations is an optimal step

toward altering surface properties, thus enhancing the stability of the colloids in organic solvents [39].

18.3.2 Surface Modification of Inorganic Nanoparticles

Premodification of the nanoparticle surface is frequently applied. There are several reasons why particle modification is performed:

- To improve colloid stability and alter particle surface properties
- To control or regulate dye adsorption
- To prevent or reduce dye molecular aggregation

Surface modification for the reduction of dye molecular aggregation is analyzed in Sect. 18.4.5. Improvements in colloid stability are often related to the modification of surface charge or the exchange of counterions. Surface grafting with molecules bearing ionic groups attached to the surface via covalent bonding can lead to significant changes in surface properties (see Sect. 18.3.4). In principle, dye adsorption itself also leads to a modification of surface properties. Thus the selection of an appropriate dye can be an alternative way to improve surface properties and achieve high colloid stability. For example, the adsorption of zwitterionic porphyrin, carrying both the cationic pyridinium and anionic carboxyl groups in the molecule, led to a significant stabilization of Mmt colloids [40]. Even the large-scale adsorption of this dye beyond the *CEC* value did not lead to particle flocculation.

The adsorption of organic ions of the opposite charge to that of the surface is often an irreversible process. However, the repulsive forces would prevent the adsorption of dye ions with the same charge. In such cases, surface modification is necessary and often realized by using ionic surfactants. The most typical examples are LSil modified with alkylammonium cations. The formed materials exhibit enhanced surface activity, and are able to absorb cations, neutral molecules as well as anions. For example, such modifications applied to Mmt turned this material into an efficient adsorbent of the anionic dye methyl orange [41]. Another type of surface modification involves surface activation with polyelectrolytes. The adsorption of organic polycations onto nanoparticles with a negative surface charge can significantly reduce or even reverse the original charge to positive values, thus creating an adsorption capacity for anionic organic dyes [42]. Applying the modification of Mmt surface with the polycation led to an increased adsorption of anionic dyes, but also retained the properties for an efficient adsorption of cations [43]. The efficient adsorption of anionic dyes on LSil can be achieved via modification with inorganic polycations or oligomeric cationic species, such as the *Keggin cation*, $Al_{13}O_4(OH)_{24}(H_2O)_{12}^{7+}$. The modification of smectites leads to materials called *pillared clays,* which exhibit enhanced porosity and interesting adsorption properties. Al^{III}-pillared clay (with *Keggin cations*) exhibited an

improved adsorption of Acid Turquoise Blue [44]. A similar trend was observed for the adsorption of orange II on silane-activated Al^{III}-pillared Mmt [45]. Besides the adsorption of anionic species, pillared clays are still able to also readily absorb cationic dyes [46], which is a similar feature to the materials modified with organic polyelectrolytes. There are some other interesting properties which have been observed for these materials: The adsorption of the cationic dye methylene blue (MB) on Fe^{III}-pillared LSil could be controlled by an external magnetic field [46]. In another study, surface modification with oligomeric cationic species led to enhanced fluorescence compared to non-pillared LSil [47].

18.3.3 Hybrids with Neutral, Insoluble, and Hydrophobic Dyes

The poor solubility of neutral and hydrophobic dyes sometimes complicates their application. Furthermore, organic nonpolar dyes which are poorly soluble in water exhibit low photoactivity in aqueous solutions. As was mentioned above, the modification of the particles with surfactants may significantly increase the adsorption of neutral dye molecules. The synthesis of hybrid materials with hydrophobic dyes must be often performed in organic solvents and/or under specific conditions to enhance dye's solubility. However, there were some recent studies which applied layered nanoparticles for dye solubilization. For example, synthetic LSil of a Lap type was used to solubilize the neutral dyes Nile red and coumarin 153 (Fig. 18.2) [48]. The co-adsorption of organic quaternary ammonium

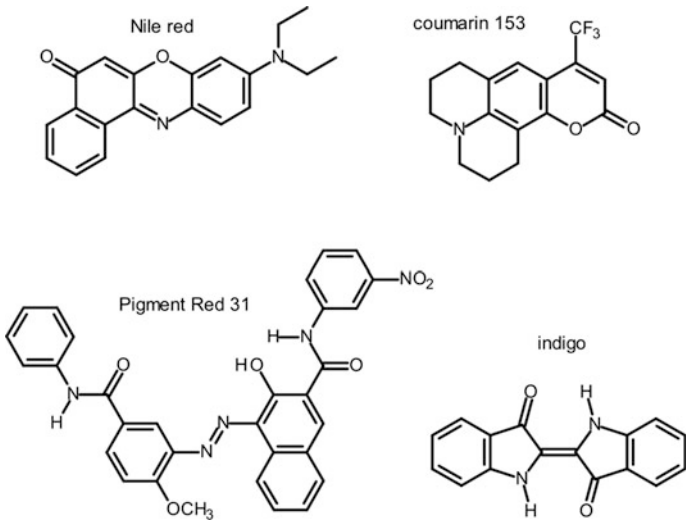

Fig. 18.2 Molecular formulas of neutral dyes used in hybrid materials

ions further enhanced dye luminescence. The small size of Lap particles guaranteed the high transparency of hybrid colloids. The stability of the hybrid dispersions remained even at higher concentrations, which indicated this material to be applicable in biophotonics [48]. The mechanism of dye solubilization in the presence of nanoparticles has not been explained yet. Theoretically there could be two different mechanisms:

1. The neutral molecule could hydrolyze, and ionized forms can be adsorbed onto the surface of opposite charge. One possible example is the reaction of the dye molecule as a Brønstedt base:

$$\mathrm{Dye\,(s) + H_2O\,(l) \rightleftarrows HDye^+\,(aq) + OH^-(aq)}$$

The cations formed would be significantly more soluble than the neutral molecules and would be selectively adsorbed on the particles with negative surface charge ($Surf^-$):

$$\mathrm{Surf^-(s) + HDye^+\,(aq) \rightleftarrows Surf^- - HDye^+\,(s)}$$

2. Poorly soluble dyes in their neutral molecular form can be stabilized in the adsorbed state to reduce hydrophobic interactions with water molecules. Thus, the stabilization of dye molecules by adsorption would be in principle the same as the precipitation of the insoluble dye molecules. Besides van der Waals forces, H-bond formation can be very important as was proven for indigo bonding in the Maya blue pigment [49]. Inspired by Maya blue, an aqueous colloid of synthetic Sap was used to dissolve the hydrophobic dye Pigment Red 31 (Fig. 18.2) [50]. The dye was bound onto the external surface via van der Waals and H-bonds but also hydrophobic interactions between the dye molecules were observed. Although no measurable intercalation of the dye was detected, the hybrid pigments were highly dispersible in water, thermally stable, and resistant to ultraviolet (UV) radiation [50]. For larger polymeric pigments, a basic solubilization route may not be efficient and special methods had to be developed. One example is a red pigment based on the large protein complex naturally occurring in red algae, called phycoerythrin. Salt-assisted adsorption promoted the fixation of phycoerythrin onto a Mmt surface [51]. In summary, the solubilization by nanoparticles seems to be very efficient for common hydrophobic dyes. This procedure can expand the use of the majority of dyes based on neutral molecules for photonic applications [52].

18.3.4 Sol–Gel Processes and Covalently Attached Dye Molecules

Hybrid materials are mostly prepared starting from the systems of both the components: Layered nanoparticles and organic dyes. However, in some cases, the syntheses of hybrid material and the formation of nanoparticles is realized in a single-step procedure. The accommodation of organic dye molecules proceeds at the same time or immediately after the formation of nanoparticles. This can be achieved relatively simply by including organic dye molecules in the mixture for nanoparticle synthesis. The earliest work using this strategy reported the formation of the hybrids based on Lap and LDH [53]. The hybrid materials with Lap particles were prepared in the course of Lap hydrothermal synthesis starting with SiO_2, $Mg(OH)_2$, LiF, and including either cationic dye alcian blue or neutral molecules of 15-crown-5-tetra-substituted phthalocyanine. The hybrids with LDHs were prepared via the hydrolysis of solutions containing $Al(NO_3)_3$, $Mg(NO_3)_2$, and NaOH, together with Cu^{II}-phthalocyanine anions. The syntheses of hybrid intercalation compounds were successful and the properties of the products were similar to those prepared by the conventional method based on ion exchange reactions [53]. The sol-gel processes are suitable routes for the incorporation of reactive dye species in hybrid materials. The dye moieties can be directly incorporated in the hybrid structure or linked via covalent bonds to nanoparticles. Trioctahedral synthetic LSil was synthesized from SiO_2, $Mg(OH)_2$, and LiF solutions together with a reactive silane molecule, carrying a coumarin dye moiety [54]. The incorporation of the coumarin fluorophores was proved by spectroscopy methods. In a similar approach, palygorskite modified with 3-aminopropyl triethoxysilane was applied as an efficient substrate, binding to specific reactive dyes [55]. In another study, a hybrid material carried two different dyes; each dye component was bound in a different way [56]. One was incorporated into the silicate matrix by hydrothermal synthesis as described in a previous work [54], and the second dye was additionally integrated by an ion exchange reaction. Förster resonance energy transfer (FRET) between these two dyes indicated a homogeneous distribution of the fluorophores in the matrix of the hybrid material [56, 57].

LSil are a typical example of the materials based on inert and chemically very stable particles. The particles edges represent a very small fraction, but with relatively reactive sites of hydrolyzed broken bonds. The high reactivity of the edge sites was utilized in another strategy for hybrid materials' preparation. The edges of LSil particles were selectively modified with reactive silane molecules bearing fluorophoric groups (Fig. 18.3) [58]. Since the particle edges represent only a minor fraction of the total surface, their modification did not significantly influence the colloid properties of the materials. On the other hand, the modification of the edges led to solid materials exhibiting relatively strong luminescence. Specific localization of the fluorophoric groups could be observed by confocal fluorescence spectroscopy only with the hybrids derived from LSi with relatively large-diameter particles [58]. Kaolinite is an LSil which neither swells nor forms stable colloids in

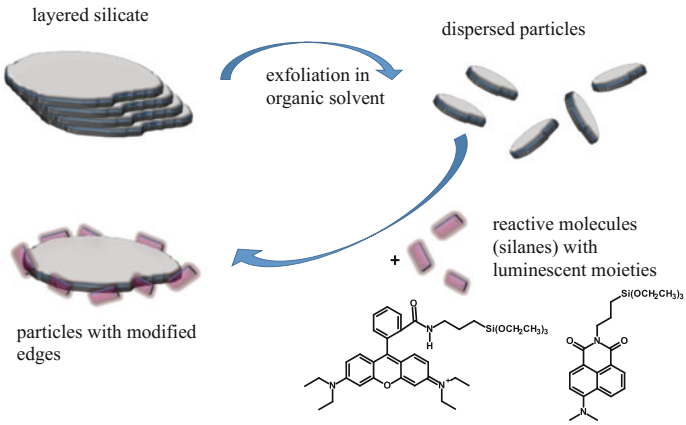

Fig. 18.3 Selective modification of particle edges with luminescent molecules. (According to reference [58])

water. Its particles do not carry any charge, so modification via ion exchange reaction cannot be applied. Therefore, hybrid materials based on kaolinite and organic dyes are rather very rare. It was reported that the microwave activation of kaolinite led to a material which exhibited better adsorption for tartrazine dye [59]. However, modification with reactive organic dyes seems to be the most affordable way [60]. After the pre-expansion of kaolinite with an organic polar solvent, the luminescent silane molecules reacted with surface OH groups leading to a unique photoactive material [60]. A very interesting but structurally complex type of hybrid material was synthesized from spherical silica particles of a submicrometer size [61]. Hydrothermal treatment with LiF and $MgCl_2$ created LSil particles attached by their edges to the silica surface. Extraordinary colloidal properties were controlled rather by the properties of silica spheres, but their adsorption properties were significantly influenced by the attached LSil particles. The modified spheres were active in the adsorption of cationic surfactant and organic dye, MB (Fig. 18.4). The colloidal stability was kept unchanged even under conditions of complete saturation with the dye cations. Under identical conditions basic hybrid MB/LSil colloids would be very unstable and completely flocculated [61].

18.3.5 Thin Solid Films

Films of hybrid materials can be used as the components in optical devices or for other numerous applications and therefore have received a lot of attention. The films based on the layered nanoparticles with organic dyes can be prepared in various ways. The simplest method is based on casting the colloids of nanoparticles on some sort of flat substrate and let the solvent evaporate out. The particles can be

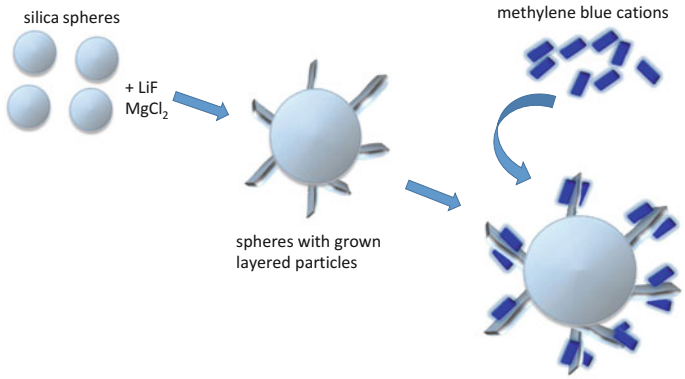

Fig. 18.4 Particles of layered silicate attached to silica *spheres* and methylene *blue* adsorption. (According to reference [61])

modified with dye molecules either already in the colloids, or in the latter step via the intercalation into the film. The most important properties which are usually required for hybrid optical films are optical homogeneity and transparency. These requirements initiated the development of various more sophisticated techniques. A spin coating and film formation via a vacuum filtration method [62] can be used for the preparation of relatively thick, but optically homogeneous and transparent films. In these cases particle size plays a significant role. Special types of films have been developed in order to precisely control composition, film thickness, structure, arrangement, and order of the discrete layers and components. These include Langmuir–Blodgett (LB) films and layer-by-layer (LbL) assemblies. Thin layers of monomolecular assemblies of amphiphilic molecules with well-defined structure and composition are basic building blocks for LB films. The assemblies are formed at an air/solution interface, from where they are deposited onto the substrate by dip coating. It is relatively simple to incorporate layered nanoparticles into LB films. Most frequently nanoparticles are modified with amphiphilic surfactant counterions; the same surfactants which are used for common LB films. The incorporation of organic dyes into LB films can be achieved in two different ways (Fig. 18.5): 1. Dye molecules are adsorbed onto the active surface of modified nanoparticles [63]. 2. Another way is to incorporate dyes molecules or ions with long alkyl chains instead of a fraction of the surfactant molecules during LB assembly. Octadecyl-Rh B or 3,3′-dioctadecyl oxacarbocyanine dye are examples of amphiphilic cations having chromophoric cationic groups, which have been applied in the production of LB films with LSil [64]. The structure of surfactant assemblies and the orientation of surfactant molecules in a hybrid LB film are similar to the films built from surfactant molecules alone (Fig. 18.5). The self-assembly of surfactant molecules and formation of dye molecular aggregates play significant roles, affecting the

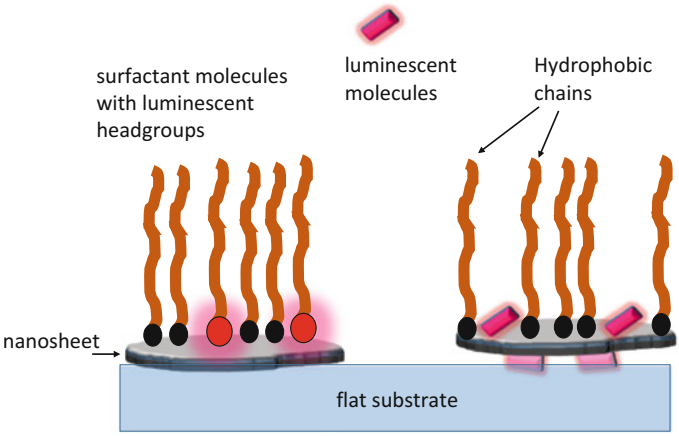

Fig. 18.5 Types of Langmuir–Blodgett films with organic dyes

optical properties of the films [65]. The influence of the surface charge density of LSil on the properties of hybrid LB films was also reported [64].

The LbL assemblies consisting of multilayers with alternating charge were discovered relatively recently. They are built via a step-by-step routine, through the deposition of a single monomolecular layer in each deposition step. The new layer with the opposite charge to the outer layer of the substrate is deposited from solution and the excess of molecules or particles is washed out after each deposition step. Coulombic forces play a key role, but other types of chemical bonds can also take a part. LbL assemblies are built by full control over the composition and order of the layers. Although the LbL technique was originally developed for the deposition of electrolytes, charged layered nanoparticles are ideal components for the multilayers of this type. The choice of the components can significantly affect the photoactivity of embedded dye molecules. For example, the dimerization of acridine orange incorporated in LbL films was significantly reduced when Lap was included in the films [66]. A detailed study utilizing chemometric analysis of the spectral data recorded after each deposition step could identify variable phenomena occurring during LbL assembly formation [67]. The outer surface with the adsorbed dye molecules exhibited significant changes upon the formation of a new layer. There was a partial desorption and conversion of dye molecules to an aggregated form. Complex and specifically designed LbL films were prepared for the purpose of investigating FRET between layers [67]. In another study, chromophoric groups were part of the polyelectrolyte chains used as the components in LbL assemblies [68]. They formed the J-aggregates exhibiting the properties of light-harvesting and excitation energy transfer systems.

18.3.6 Nanocomposites with Polymers and Other Complex Systems

More complex hybrid materials including industrial polymers were also developed. Nanocomposites of LSil particles with poly(styrene) and Rh 6G were synthesized in a two-step process [69]: First, the dye and radical initiator 2,2,6,6-tetramethyl-1-piperidyloxy (TEMPO) were intercalated in LSil. The addition of styrene and TEMPO-initiated polymerization led to polymeric nanocomposites that stabilized incorporated Rh molecules [69]. Spherical particles of poly (*N*-isopropylactylamide) hydrogels containing layered particles of Sap were used for the immobilization of various cationic species, including organic dyes [70]. Oligomeric silsesquioxane with a covalently attached chromophoric group of luminescent cyanine dye was intercalated in synthetic Sap. The hybrid material exhibited a high luminescence quantum yield and improved thermal and photochemical stability. The hybrid exhibited superior properties with respect to the luminescent oligomer or dye molecule alone [71]. In another study, hybrid mesoporous materials with high surface area were synthesized from LSil and poly (ethylene glycol) grafted sol–gel silica. The aerogel formed by evaporating the solvent exhibited hydrophobic properties, but with high capacities for the adsorption of ionic organic dyes, MB and malachite green [72]. Very interesting optical materials were developed when incorporating gold nanoparticles in LDH, exhibiting superior properties to adsorb methyl orange [73].

18.4 Molecular Aggregation and Photoactivity of Hybrid Materials

18.4.1 Metachromasy and Dye Molecular Aggregation

The discovery of dye molecular aggregation represents one of the most important milestones in the physical chemistry of organic dyes. The molecular aggregation of some organic dyes causes metachromasy, which was originally defined as significant color change induced by changing conditions, such as temperature, ionic strength, concentration, adsorption, etc. For the first time metachromasy was visually observed by optical microscopy in biological tissues stained with metachromatic dyes. The spectral changes often cover the complete range of the visible spectrum, sometimes representing spectral shifts of several thousand cm^{-1}. Exciton theory describes the spectral changes as the result of the electrostatic coupling between transition dipoles of dye molecules. It significantly alters the electronic properties of the dye molecules, namely the energies of their excited states. The dipole coupling depends significantly on the geometry of the aggregates

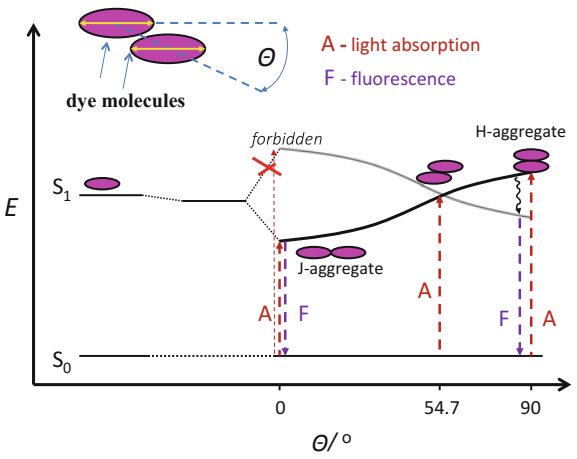

Fig. 18.6 Exciton splitting of the electronic excited states of dye molecular aggregates

(Fig. 18.6). The H-aggregates with the geometry characterized with a sandwich-type arrangement exhibit absorption bands shifted to lower wavelengths. The H-aggregates are mostly nonluminescent and nonactive species and often exhibit the properties of fluorescence quenchers. J-aggregates represent the type of molecular assemblies with a head-to-tail intermolecular association. They are characterized by light absorption at longer wavelengths, narrow absorption bands, and exhibit relatively small Stokes shifts. The J-aggregates represent interesting supramolecular systems with a broad spectrum of potential applications [74]. The formation of dye molecular aggregates on layered nanoparticles is a relatively common phenomenon. Probably one of the first papers reporting dye molecular aggregation in such systems was on MB in Mmt colloids [75]. The main driving force for dye aggregation is hydrophobic effect and enhanced concentration at liquid/solid interface. There are two main types of sites for dye aggregation: 1. The zones of the diffuse electric double layer surrounding colloid particles. 2. Sites at the particle surface. The zones with enhanced electrolyte concentration and ionic strength promote initial dye aggregation. The thickness of the zones and electric field characteristics depend on the charge of the particles and electrolyte type and concentration. Particle edges do not seem to play a significant role in dye adsorption and molecular aggregation, since they are a minor part of the total surface. The chemical modification of LSil particle edges with reactive silanes did not produce different tendencies in MB aggregation, although the properties of the colloids were significantly altered [76]. The planar surfaces of layered particles can exhibit variable properties, specific charge, topography, and chemical activity. Therefore the mechanism of dye aggregation is relatively complex, including fast adsorption and slow processes of the transformation of initially formed metastable dye aggregates [27, 77–79].

18.4.2 Molecular Aggregation and Photoactivity

Dye aggregation significantly affects the photoactivity of the molecules. As was mentioned above, most common aggregates are sandwich-type assemblies exhibiting low photoactivities. Therefore, the adsorption of dye molecules onto layered particles often leads to a decline in their photophysical properties. This phenomenon has been described in numerous articles and reviews [9, 12, 15, 80, 81]. However, there have been a few reports of an opposite trend. This may occur if the dye adsorption does not lead to molecular aggregation. Rarely dye adsorption can even suppress the formation of dye aggregates. This phenomenon occurs for organic dyes of specific molecular structure and the distribution of ionic groups in their molecules. For example, the aggregation of Sb^{V}-porphyrin was suppressed and fluorescence increased in the complexes with LSil. This effect was observed even at high loadings of the porphyrin dye [82]. In a few cases, the formed aggregates can be photoactive (e.g., J-aggregates or other specific types) (see Sect. 18.4.4). For example, the aggregation of cationic p-phenylene ethynylenes on Lap particles led to an enhanced fluorescence. The effect of the layered particles was to minimize the interactions of the dye molecules with water [83]. In some cases, the bonding between the adsorbed dye molecules and particle surface suppresses the mobility of dye molecules, thus reducing their quenching via collision frequency and other unfavorable relaxation pathways [84]. For example, the adsorption of cationic porphyrazine dye on inorganic nanosheets with negative charge led to a strong enhancement of their fluorescence quantum yields and lifetimes of their excited states. The phenomenon was named "*Surface-Fixation Induced Emission*" [85]. Another example is diarylmethane dye, auramine O, which exhibited enhanced fluorescence in Mmt colloids. The adsorption of this dye led to minimizing relaxation pathways via restriction of the torsional molecular motion [86, 87]. In the strategy to reduce molecular aggregation, layered particles were compared with other substrates. Nanosheets, being more rigid substrates, in some cases exhibit better properties for reducing dye aggregation than polymeric compounds [88]: Cyanine dye exhibited strong aggregation on negatively charged polymeric templates such as substituted amylose and cellulose. Substantially less aggregation was observed in the systems with lower negatively charged templates such as hyaluronic acid. Adsorption on Lap particles did not lead to dye aggregation, thus exhibiting optimal properties [88]. In rare cases, H-aggregates exhibit strong luminescence. One example is the H-aggregates of 3,3-dioctadecyl oxacarbocyanine dye formed in Lap colloids. The dye aggregates exhibited high activity in energy transfer processes [89]. The adsorption taking place in aqueous colloids of layered nanoparticles often leads to increasing solubility of poorly soluble, hydrophobic and nonionic dyes as has been discussed above (see Sect. 18.3.3). Neutral dye adsorption also leads to the reduction of dye molecular aggregation [48, 90, 91].

18.4.3 *Effect of Layer Charge*

The molecular aggregation of organic dyes significantly depends on the charge distribution on the nanoparticle surface [12]. For the first time, the effect of the layer charge was observed for MB using reduced-charge montmorillonites (RCMs) [27]. The series of RCMs was prepared from a single parent material saturated with Li^+ cations. The charge was reduced upon the fixation of Li^+ cations in layers by heating. The extent of the charge reduction was proportional to the temperature used in the thermal treatment. The samples of RCMs in a single series are very similar in structure, composition, and particle size and shape, but different in the layer charge and related properties. It is interesting that only very small, almost negligible changes in the layer charge led to significant changes in molecular aggregation [27, 92, 93]. With decreasing layer charge, H-aggregation decreases in favor of monomers, H-dimers and J-aggregates. There could be two interpretations of this phenomenon:

1. Low charge density on the particle surface induces larger distances between the adsorbed neighboring dye cations. This would suppress dye aggregation. High-charge density is reflected in small distances between adsorbed dye cations balancing the surface charge. This would promote the formation of H-aggregates.
2. Layer charge affects the electric double layer in the vicinity of the particle surface. High-charge density induces a high concentration of ions on the surface, and a high ionic strength which contributes to the increase in electric field. The increase in the ionic strength and high concentration of electrolyte ions would support the formation of dye molecular assemblies. The effect of ionic strength was proved in MB aggregation in Mmt and Lap aqueous colloids [94], and has also been observed for the dye aggregation in solutions.

The trend of the effect of the layer charge observed with the series of RCM samples was later confirmed with a series of various LSil, including samples of both natural origin and synthetic materials, of di- and trioctahedral structure, with the location of the charge due to substitutions in the octahedral or tetrahedral sheets [12, 28, 87, 95, 96]. The high sensitivity of the dye molecular aggregation to the layer charge was taken advantage of in layer charge probing. The method was successfully used to measure charge reduction due to cation fixation or induced by acid treatment [28, 97]. The effect of the layer charge is a general phenomenon, regardless the type of organic dye. It has been observed for the aggregation of MB, other phenothiazines, triphenylmethane and xanthene dyes, and oxazines. There is no simple model to describe the effect of the layer charge on the formation of J-aggregates [98]. These assemblies are structurally relatively variable and their formation is predominantly influenced by the dye molecular structure. J-aggregates are preferentially formed with dyes with a complex molecular shape, nonsymmetric position of the charged and polar groups, etc. (see Sect. 18.4.4).

An appropriate selection of layered templates, preferably with a low layer charge, is a basic precondition to avoid or at least to reduce dye molecular aggregation in hybrid materials. The appropriate choice of organic dye without metachromatic properties is another strategy being widely applied. Takagi and his coworkers elaborated on the optimal selection of suitable porphyrin dye/LSil pairs to obtain materials with optimal photophysical properties and high photoactivity. Both the dye and LSil templates were selected to match the charge distribution in both the components, so that the dye molecules would form a dense occupation on the host surface, but avoiding any molecular aggregation. There are specific guidelines which can be useful for selecting appropriate components and designing the composition of active and functional hybrid materials. These guidelines are called the *Size-matching rules* [40, 99–101] and reflect the matching the structural properties of both the dye and layered substrate.

18.4.4 J-Aggregates

A lot of attention has been devoted to J-aggregates due to their unique properties [74]. Their formation is not as rare and depends greatly on the conditions and dye molecular structure. The J-aggregation of cationic dyes has been studied more frequently, but it has been also observed for anionic dyes (e.g., [102]). As was mentioned above, J-aggregates are recognized by light absorption at lower energies. However, the adsorption of organic dye molecules itself is frequently accompanied by the same spectral shift [103]. Also conformational isomerization in the molecules occurring upon dye adsorption causes the same spectral changes [104] (see Sect. 18.5.2). J-aggregation was frequently also confused with the protonation of dye molecules [12]. Therefore, it is sometimes difficult to recognize if the spectral changes are due to J-aggregation. Rh dyes are a typical example [79], since there is only a small energy difference between the transitions of the monomeric form and J-dimers. Nevertheless, there is clear evidence of the formation of J-aggregates in numerous hybrid systems. J-aggregates are easily formed with dyes which have molecular shapes inappropriate for the formation of sandwich-type molecular assemblies. These mostly include cyanine dyes with side chains near the molecular center or porphyrins with a specific molecular shape and distribution of ionic groups [98, 105–107]. There are two types of J-aggregates. Ideal J-aggregates with a perfect head-to-tail association exhibit light absorption at lower energies, whereas so-called oblique aggregates are characterized by both H- and J- spectral bands. Both types of J-aggregates can coexist in some systems. An example is the two types of J-aggregates of pseudoisocyanine dye recognized in LSil films [107]. J-aggregation can be easily achieved for dyes whose molecules bear both positively and negatively charged groups. The charge distribution in zwitterionic molecules prevents a sandwich-type stacking. Examples are porphyrins with cationic pyridinium and anionic carboxyl groups in their molecules [40]. The formation of

J-aggregates can be significantly influenced by the third components in more complex systems, such as in LbL assemblies [67] or in systems with polymers [108].

18.4.5 Reduction of Dye Molecular Aggregation by Using Surfactants

The purpose of using surfactants is to dilute the adsorbed dye molecules and thus to achieve the suppression of dye molecular aggregation. There are several works providing evidence on the important role of ionic surfactants in improving the photophysical properties of hybrid materials. Cationic surfactants are used for nanoparticles with a surface negative charge [33, 109]. For the modification of nanoparticles with a positive charge, anionic surfactants are used [110, 111]. A series of materials based on LDH, anionic dye (1-anilinonaphthalene-8-sulfonate), and alkylsulfonate surfactants with variable length of alkyl chains were prepared and characterized [111]. Their luminescence depended on the structure of the formed assemblies, which sensitively reflected the properties of the surfactant used. Optimal conditions were found by combining the appropriate dye loading and proper selection of surfactant. Under optimal conditions, no apparent quenching took place for dye loading up to 20% of the anion exchange capacity of LDH [111]. Much lower dye concentrations were needed to completely avoid dye aggregation in the hybrid materials of Mmt modified with cationic alkylammonium surfactants. Optimal Rh dye loadings were only 0.1-0.5% of *CEC,* but fluorescence quantum yields achieved up to 80% under the optimal conditions [112, 113]. The properties of the molecular aggregates formed at higher dye loadings were also improved. They exhibited significant luminescence, in contrast to the aggregates formed in the absence of the cationic surfactants [114, 115]. The use of the surfactants does not always guarantee improved properties. In some cases, the modification with surfactants leads to an increase in molecular aggregation. For example, the interactions of anionic Merocyanine 540 in bentonite premodified with cetyltrimethylammonium cations led to the formation of H-aggregates with reduced photoactivity [116]. In another study, a higher fluorescence of hybrid films was achieved without a surfactant [117]. On the other hand, aqueous colloids of the same components exhibited an opposite trend. The effect of the surfactants probably depends significantly on the procedure used for hybrid material synthesis and on the type of material. There are several possible explanations for the opposite effect of alkylammonium cations. One is based on the phenomenon of molecular segregation. The formation of a segregated phase of alkylammonium cations reduces the surface available for the segregated dye molecules. As a consequence, the segregation leads to a locally increased concentration of dye molecules, thus promoting their aggregation [118]. This segregation was also proven for systems based on a mixture of different organic dyes. An example is a mixture of porphyrin and viologen dye co-adsorbed on Sap particles [119]. The fractions of each dye formed segregated phases, each

composed of a single type of molecules. The different structures of porphyrin and viologen molecules contributed to the increased stabilities of the segregated phases and prevented the formation of the mixed phase. The segregation was proven by energy transfer experiments. Part of the segregated porphyrin molecules remained luminescent and could not participate in the FRET process that would quenched their fluorescence with viologen [119]. The segregation can also be induced by reaction conditions affecting the properties of hybrid systems with ionic surfactants. For example, the effect of alkylammonium cations in solid hybrid systems depends significantly on the ambient humidity, as was observed for Rh 3B intercalated in LTi [120]. Water adsorption leads to the formation of dye molecular aggregates and significantly reduces the material's luminescence. The effect of humidity can be explained by a hydrophobic effect which arises with increasing water content. The presence of water molecules contributed to the self-assembly of alkyl chains forming a compact, isolated phase, thus pressuring the dye molecules to segregate from the alkylammonium phase.

18.4.6 Molecular Aggregation in Other Systems

Another strategy to prevent molecular aggregation was based on using a type of organic compound with 'container-shaped' molecules, called cavitands. Cavitand molecules have cavities which can accommodate single dye molecules inside, thus preventing their association. Dye/cavitand complexes could be adsorbed onto layered nanoparticles in similar ways to dye molecules alone. The effectiveness of the strategy to minimize molecular aggregation has already been proved. Cationic Zn^{II}-porphyrin, and 2-acetylanthracene encapsulated within a cationic organic cavitand were adsorbed on LSil particles. The hybrid exhibited high photoactivity, and the FRET efficiency between the dye components reached almost 100%. It proved a uniform and nonsegregated distribution of porphyrin cations and cavitand complexes [121]. In a similar way, cyclodextrine molecules with cavities which can accommodate luminescent dye molecules were also applied in hybrid films to prevent molecular aggregation [122]. There are several papers reporting the influence of polymeric substances on dye molecular aggregation. For example, interesting materials were prepared from oxazine 1 and in situ formed poly(norbornane) and fluoromica nanoparticles [108]. The co-adsorption of polar copolymers of poly (ethylene oxide) and poly(propylene oxide) on Lap led to enhanced dye aggregation. It is likely that segregation occurred between the polymer molecules and dye cations. Interestingly, the dye adsorption on Lap without polymers led to lower dye aggregation [123]. However, an opposite trend was observed for the particles modified with water-soluble chitosan. The presence of the polymer changed the dielectric properties near the adsorption sites, thus reducing molecular aggregation and increasing the fluorescence of the hybrid material [124]. Enhanced fluorescence was also achieved in the hybrid materials modified with the cationic polyelectrolyte [125].

18.5 Phenomena and Properties of Hybrid Materials

18.5.1 Optical Anisotropy and Dye Molecular Orientation

The term *anisotropy* refers to material's properties which are directionally dependent. Optical anisotropy defines the optical property of a substance that depends on the direction of light propagation or polarization. Nanosheets or nanolayers are anisotropic materials which result directly from the structure and shape of the particles. The aspect ratio of these materials is a parameter which quantifies the geometric shape of the nanoparticles, and is defined as the ratio of the particles' diameter to the thickness of an individual particle. The layer thickness is mostly well defined, resulting from the structure of a specific compound and generally does not exceed a few nm. There is a large variation in the diameter of the particles, being in the range from tens to hundreds of nm. Nevertheless, the aspect ratios of the particles of layered compounds is mostly well above 10, which significantly affects the association of the particles in colloids or in the solid state. Face-to-face assemblies with the particles aligned in a parallel fashion are preferentially formed in the solid state. The nanoparticles forming films are oriented in a parallel fashion with respect to the substrate surface plane. Such an orientation has a high impact on the material's optical anisotropy. The molecular orientation of dye cations depends on many parameters and conditions, such as molecular shape and the distribution of ionic and polar groups [126, 127], concentration [33, 126], and molecular aggregation [12, 93], which is controlled by the surface properties of the nanoparticles [30]. The probability of the absorption of electromagnetic radiation by chromophoric groups depends on the orientation between the electric vector of the light and the transition dipole moment of the chromophore. The orientation of the transition dipole moment in molecules is determined by the electronic structure of the chromophores. The direction of the electric vector is perpendicular to the propagation direction of the light. Polarization can be achieved using polarizers. Optical anisotropy can be characterized by combining polarized light and control of the orientation of the film with respect to the light's propagation. In principle, the two-dimensional character of nanosheets and layers do not allow a perfect preferential orientation of the dye molecules in all three space directions. However, three-dimensional anisotropy can be achieved using a monocrystal of layered host material with an ordered structure in all directions, such as $K_4Nb_6O_{17}$ [128].

There have been several attempts to characterize the molecular orientation of dye molecules in layered compounds. A parallel molecular orientation of dye molecules on the surfaces was most frequently considered, since it would contribute to the highest interaction area between the particle surface and dye molecules (see references in [12]). However, the Coulombic interaction between the surface and dye ions controlling dye molecular orientation depends greatly on the distribution of electron density in the molecule. Optical anisotropy obtained with X-ray photoelectron spectroscopy on well-defined systems based on mica and MB [129] and triphenylmethane dyes, crystal violet, and malachite green [130] determined an

inclined, almost perpendicular orientation of the molecules. The molecular orientation significantly depends on dye loading [126]: At low dye loadings the dye molecules lay flat on the surface. With increasing concentration there was a continuous change in the average molecular tilt angles to larger values. The perpendicular orientation of cationic laser dyes Rh 6G and oxazine 4, incorporated in an oriented film of synthetic fluoromica, was observed by polarized IR and UV-VIS absorption spectra [32]. A significant proportion of the dye cations assigned to aggregates were tilted, with the longest axis of the heteroaromatic ring nearly perpendicular to the host layer, and exhibited a positive optical dichroism. The spectral properties of ionic phthalocyanines intercalated into Hec and LDHs using various synthetic routes were compared [53]. The dye molecules were oriented parallel to the surface of Hec but exhibited a perpendicular orientation in LDH hybrid materials. The different orientation was assigned to the much higher layer charge of LDH, and higher density of intercalated dye anions in the interlayer spaces [53]. The orientation of tetracationic porphyrins in α-zirconium hydrogen phosphate with high layer charge was relatively inclined [131], although the parallel orientation was observed for the same dyes in the hybrids with LSil [132]. Large planar Cu^{II}-phthalocyanine tetraanions intercalated in layered $Cu_2(OH)_3CH_3CO_2$ were arranged with the orientation of the molecular planes perpendicular to the surface of $Cu_2(OH)_3^+$ layers [133]. The effect of the layer charge on dye molecular orientation was proved for Rh 6G cations in the films of RCMs: [29]. In contrast to the H-aggregates, the molecules forming J-aggregates were oriented more or less in parallel and had no tendency for perpendicular orientation [107]. On the other hand, the J-aggregates formed on layered particles exhibit negative dichroism [106–108, 117, 134]. Several studies found the hybrid systems to exhibit fluorescence anisotropy [15, 135, 136], although fluorescence cannot detect inactive species, such as H-aggregates. No significant depolarization due to the rotational relaxation of the fluorophores was observed in the solid hybrid films. Fluorescence anisotropy of the material proved a rigid association of the fluorophore molecules with the host surface [137–140]. However, some phenomena such as resonance energy transfer can lead to a partial or complete light depolarization [117, 140].

Whereby the orientation of layered particles in the films is achievable relatively easily, colloids are relatively isotropic systems with a random orientation of particles. On the other hand, the orientation of the chromophores in colloids can sensitively reflect the properties of the solvents, which can be important in various applications, such as for optical sensors or switches [141]. Electric linear dichroism is a phenomenon characterized by the anisotropic absorption of light under an externally applied electric field. The effect of the electric field is to induce a preferential orientation of the colloidal particles with respect to the direction of the field. Electro-optical properties have only been described for a few hybrid colloids [135, 142].

Optical anisotropy, birefringence, and linear dichroism are very important optical parameters. However, in some cases they can influence other properties.

One of the most interesting examples is the light-induced deformation of poly-(*N*-isopropylacrylamide) gels, which was mediated by LSil particles with adsorbed porphyrin molecules [143]. The alignment of the nanosheets in the gel was achieved by an electric field applied during polymerization to form optically anisotropic materials. When the gel was irradiated with light, only the colored part was photothermally deformed, which was followed by anisotropic shrinkage. The direction of the shrinkage was dependent on the orientation of the layered particles [143].

18.5.2 Structural Changes and Photochromic Properties

Conformational changes in molecules are realized by rotations around single bonds and do not require much energy. Dye molecules in the adsorbed state may have geometries different from those in solution. A typical example is the adsorption of porphyrin derivatives having cationic *N*-methylpyridinium substituents [104]. In solutions, the pyridinium groups in the molecules are inclined with respect to the plane of porphyrin ring. However, the inclined groups would not efficiently bind to the surface in the adsorbed state. Therefore, rotation of the pyridinium groups often occurs depending on the location of the methyl substituent and positive charge. Porphyrin with *N*-methyl-4-pyridinium groups (*ortho* substitution) have to rotate to an almost completely parallel orientation. Such conformational change leads to an overall flattening of the porphyrin molecule [144]. The extended conjugation of the π electron system in the planar molecule contributes to a reduction in the energies of both light absorption and emission. Spectral changes are significant and comparable to those induced by molecular aggregation. The combination of chemical modification, reaction conditions, molecular aggregation and conformational changes together can be applied to design materials with variable optical properties, but based on a single porphyrin dye [145–147]. The possible applications of such systems have been demonstrated in several papers [100, 148–150]. Recently, conformational changes were also described for the natural, luminescent dye berberine [151]. A positively charged, quaternary ammonium group is part of the dye's molecular skeleton. Partial planarization of the skeleton takes place upon dye adsorption to arrive at a more efficient electrostatic bonding, as has been proven by the systems with Sap [151].

Photochromism is the phenomenon of a reversible photochemical transformation between two isomers. The hybrid materials exhibiting photochromic properties are based on spirooxazines, spiropyrans, diarylethene, and azo dyes [14]. Photochromic materials can be used for various types of devices and industrial applications, such as optical switches, filters, light protection and photoresponsive coatings, optical data storage materials, etc. Photochromism has a reversible character; its limitations are related to the slow decomposition of the photochromic dye with the number of

applied cycles. Dye stabilization can be achieved using surfactant molecules. However, the chemical environment of the hydrophobic phase of surfactant chains can play a role in the chromophore response to photoactivation as well as in thermal relaxation of the excited molecules. Dye molecular aggregation significantly affects photochromic properties. It alters the parameters of photoactivation, but also new deactivation pathways may occur in the aggregated state. The effect of the molecular aggregation on reaction kinetics was also observed. An example is the slower formation of merocyanin from spiropyran intercalated in $MnPS_3$, due to the formation of spiropyran J-aggregates [152]. However, there are some cases where the aggregation does not significantly influence photochromic reactions. Examples are the aggregates of azo dyes exhibiting highly efficient and reversible trans-cis isomerization in hybrid materials [153–155]. The variable impact of molecular aggregation could be due to a large variation in the activation energies of photochromic reactions. For example, the formation of new constitutional isomers with new bonds and functional groups has much higher activation energies than stereoisomerization. In the former, the reactants can be stabilized in the form of molecular aggregates. On the other hand, stereoizomerization keeping bonds and functional groups unchanged have lower activation energies and could be easier to achieve regardless the occurrence of molecular aggregation. There are several reports on highly reversible photochromic hybrid materials based on nanosheets or nanolayered materials and photochromic dyes. For example, films of diarylethene/LSil hybrid materials exhibited a highly reversible decoloration of the dye. In contrast, the reaction of a dicationic derivative of azobenzene was effectively suppressed in both the colloids and films of LSil [155, 156]. Probably ionic fixation of the two cationic groups prevented dye photoisomerization. Anchoring ionic groups onto molecules and binding them on negatively charged surfaces could be utilized for the stabilization of some photolabile compounds [155]. In some cases, photochromic reactions also affect other properties. Small changes in basal spacing detected by X-ray diffraction were assigned to different arrangements and spaces occupied by different photoisomers [152, 153, 157, 158]. Another example is the reaction of spiropyran affecting the magnetic properties of the $MnPS_3$ host [152]. Interesting phenomena relate to the influence on the properties of other molecules coexisting in hybrid material. For example, the photoisomerization of diarylethene affected the molecular aggregation of cyanine dye co-intercalated into the same material [159]. The photoisomerization of azobenzene dye molecules in zirconium phosphonate, $ZrF(O_3PCH_2)_2NHC_8H_{17}$, led to their irreversible deintercalation [160]. Selective adsorption induced by the photoisomerization of azo dyes was also reported [161, 162]. The reversible cycles of adsorption or release of phenol substances could be controlled by repeated photoreaction applying UV and visible light irradiation cycles. Such materials can be used as recoverable substances for the purification of chemical wastes.

18.5.3 Nonlinear Optics

NLO properties strongly depend not only on the structure of dye molecules, but also on their bonding in the matrix of the inorganic host [163–165]. A random molecular orientation is not favorable. Optical anisotropy and preferential orientation may play a significant role in the improvement of NLO properties [166–170]. The stabilization of dye molecules in a hybrid system can also play a positive role. An essential role of dye molecular aggregation in NLO properties has also been reported. Concentration and orientation are the key factors affecting dipole-dipole interactions. For example, stilbazolium dye intercalated into layered chalkogenide MPS_3 exhibited second harmonic generation; however, this was only when in the form of J-aggregates [171]. In some cases, the structural changes to dye molecules contribute to the improvement of NLO properties in hybrid systems [168]. For example, increased molecular planarity upon the intercalation of some cationic porphyrins (see Sect. 18.5.2) can improve NLO properties [167]. An increasing concentration of hemicyanine dye in the hybrid materials with Lap altered the mechanism of the photoinduced charge-transfer process. The intramolecular mechanism taking place at low concentrations changed to the intermolecular pathway, which was reflected in a change in the NLO properties of the dye [170]. For practical use, NLO materials for optical devices must be in the form of either a single crystal or thin film. For the solid materials in the form of thin films, low light scattering is a crucial condition for successful applications [168, 172]. There are numerous examples of the construction of hybrid materials exhibiting second harmonic generation [171, 173] or two-photon absorption [62, 169]. Besides these, there are also other types, such as Langmuir monolayers or LB films [173, 174], LbL assemblies [166, 175] and nanocomposites with polymers [176, 177].

18.5.4 Resonance Energy Transfer

FRET is a phenomenon of light energy transfer taking place between two dye molecules. It can be described in two steps: 1. The dye molecule acting as the energy donor (ED) absorbs a photon and is lifted into its electronic excited state. 2. The excited molecule of ED transfers its energy to the second dye molecule, which plays the role of energy acceptor (EA). FRET is a nonradiative deactivation process, which is based on resonant electrostatic coupling between the transition dipole moments of the interacting molecules. The spectral overlap of the ED emission and EA absorption spectra is a basic condition for the resonance to take place. FRET efficiency is extremely sensitive to the intermolecular distance (1–10 nm), but also

depends on molecular orientation. Highly efficient FRET occurs in photosynthetic systems in green plants, and this phenomenon will likely play a key role in future solar cells performing at a molecular level.

Various hybrid systems exhibiting efficient FRET have been developed. The chief role of the layered particles is to concentrate the dye molecules to reach resonance. Unfortunately, an enhanced concentration of dye molecules often leads to a concurrent phenomenon - the loss of photoactivity due to molecular aggregation (see Sect. 18.4). Examples of hybrid systems exhibiting efficient FRET are LDH systems with anionic porphyrin and pyrene dye [178], or hybrids with cationic porphyrins and LSil [179]. In numerous cases, FRET efficiency achieved almost 100% [101, 150, 180]. High efficiencies were observed even with a large excess of ED molecules [180, 181]. Whereas the formation of H-aggregates is not desired, photoactive J-aggregates may play a positive role in FRET [68]. Exciton delocalization in the molecular aggregate would favor energy migration and very efficient excitation energy delivery to the EA molecules. An interesting type of molecular aggregates are mixed J-aggregates based on different dye molecules of similar structure. In such systems, very efficient *superquenchers* can accept the energy from a severalfold larger number of ED molecules. Such systems with layered nanoparticles have been only rarely investigated [182]. FRET is significantly more efficient in solid films than in colloids. In the solid phase, the process proceeds in all three dimensions, whereby in the colloids with dispersed individual layered particles, FRET is limited to two dimensions. [180]. The segregation of dye molecules can significantly reduce FRET efficiency [99]. The effect of molecular orientation has also been observed. The orientation of some porphyrin molecules intercalated in LSil responds to the solvent type. The changes in the molecular orientation responding to the presence of specific solvents makes it possible to control the FRET process by changing the chemical environment. Such systems can be used as sensors or in photofunctional devices [101, 183]. FRET in hybrid systems does not need to be limited to a single-step process. Energy migration, or two-step FRET in systems with three different dyes [140] or a multistep FRET [117] have already been reported. Besides the most common systems based on simple colloids or solid films, FRET in other types of materials have also been observed. Noteworthy examples are LB films [184–186], LbL assemblies [67, 68, 187] and others [188]. Besides the possible applications described above, FRET was found to be an extremely sensitive tool for the characterization of competitive dye adsorption on the surface of layered nanoparticles [180]. Some materials exhibiting FRET sensitively respond to pH or concentrations of various analytes [187, 189, 190]. Another type of application, which has been widely investigated, is the photoprotection of sensitive agricultural chemicals such as pesticides or insecticides. Photolabile compounds undergo easy and rapid photochemical decomposition upon solar irradiation, but FRET has been applied to slow down these processes [191–193].

18.5.5 Dye Reactions and Photosensitization

One of the major problems occurring with the applications of some organic dyes is their low photochemical stability. The stabilization of organic chromophores by the formation of hybrid systems was successfully achieved a long time ago: It was Maya blue which inspired the development of similar materials [1]. The stabilization of natural dyes can be very important in their use in the food industry and cosmetics [194]. However, the adsorption of organic dyes on layered nanoparticles does not always lead to their stabilization. For example, MB is stabilized on particles of some silicates, such as palygorskite and Mmt, but others, such as sepiolite, vermiculite and zeolite, accelerated its photodegradation [195]. It is sometimes difficult to determine which properties play a dominant role in a dye's stabilization. The stabilizing effects have been assigned to polar and ionic interactions [196], π-π interactions [194] and molecular aggregation [195]. Examples of stabilized organic dyes in hybrid systems include anthocyanin in Mmt [197], beta-carotene, and annatto dye in organically modified LDHs [194], natural anionic dyes, carmine yellow, and carthamus yellow in LDHs [196], 1,1′-diethyl-2,2′-cyanine and tris (2,2′-bipyridine)ruthenium(II)) in Sap [198], etc.

The photodecomposition of some organic dyes catalyzed by inorganic hosts has also been observed. Lap induced only a de-ethylation reaction of Rh cations, whereas the reaction with Mmt continued with the decomposition of the chromophore [199]. Photosensitization with Fe^{III} present in Mmt particles can play a role. Different pH of the colloids, layer charge, formation of reactive oxygen species (ROS), efficiency of light source; all these factors can influence dye decomposition [103, 200]. Labile dyes can be stabilized in more complex systems. For example, Rh B was unstable in polypropylene, but was stabilized in the polymer nanocomposites with Mmt particles [201]. Larger reactivity of the dyes is expected in the systems with layered semiconductors. For example, LNb played a role in the electron transfer from photoexcited Rh molecules, thus catalyzing their decomposition [202]. Therefore, using inert layered nanomaterials can be advantageous in dye stabilization.

Various dyes exhibiting properties of photosensitizers form stable triplet states upon their excitation with visible light. They are able to efficiently activate O_2 to its singlet form ($^1\Delta_g$), which can secondarily convert to other ROS. Their formation was observed in the systems based on LDH [203]. Formed $^1\Delta_g$ and ROS can efficiently accelerate the oxidative decomposition of organic compounds. The involvement of ROS in the fading of triphenylmethane dyes was observed [204]. The stabilizing effect of molecular aggregation can relate to the lower activity of dye aggregates to form triplet states [195, 205]. Another effect could be reduced diffusion rates of O_2 molecules in intercalated compounds. The hybrids with photosensitizers can be applied as disinfection materials due to their harmful activity to microorganisms. MB in the colloids of LSil exhibited high antimicrobial

activity, although dye photoactivity was significantly reduced [205]. Layered particles improved the antimicrobial effect by concentrating the photosensitizer on their surface and delivering active molecules to microbe cells. Similar materials based on LDH with porphyrin dyes were also investigated, and the formation of $^1\Delta_g$ was proven [110, 206–208]. $^1\Delta_g$ can be used as a specific oxidation agent in organic synthesis. The light-induced oxidation of electron-rich compounds, such as quinol, 1-naphthol and anthracene were mediated by hybrids with MB and Rose Bengal [209]. Some organic dyes are also reactive compounds under dark conditions, and their reactions can be initiated or catalyzed upon adsorption onto layered particles [98, 210, 211]. The bleaching of cyanine dyes in colloids was very fast with LSil with a high layer charge. The same dyes were stabilized at the surfaces of LSil with a low layer charge.

In a few cases, the reactions of organic dyes can lead to novel materials. For example, anionic azo dyes adsorbed on LDH formed highly luminescent and photostable compounds [212]. It was assumed that the reaction led to the breaking of –N=N– bond and a reactive product was chemisorbed onto the LDH surface [212]. In a similar way, UV irradiation was applied to initiate the reaction of 2-hydroxychalcones, yielding colored flavylium compounds. The products were stabilized in the matrix of Mmt modified with cationic surfactants [213]. Unique reactions of excimers or exciplex formation can be suppressed in hybrid systems [214]. Organic radicals are another type of interesting substances, having unpaired valence electrons. They are mostly unstable, but the stabilizing effect of inorganic layered hosts has been observed in numerous cases. Most often radicals or ion-radicals derived from viologen ions have been investigated. The hosts can initiate radical formation by the intercalation of reactant molecules. The inorganic matrix may also play a protective role to prevent the diffusion of O_2, which would reoxidize the formed radicals. Semiconductors such as LNb or LTi can play the role of electron donors. For example, viologen in hybrids with LTi changed to a blue radical product [215]. In other system, $Na_2Ti_3O_7$ modified with alkylammonium cations and intercalated with two cyanine dyes exhibited an electron transfer reaction. Electron spin resonance proved the formation of radical dications exhibiting high stability [216]. However, chemically inert particles of LSil were also able to promote and stabilize radical formation. Methylviologen intercalated in Lap samples converted to radicals, which initiated dimethylaniline polymerization. The polymeric product of a purple color was formed on the samples with low layer charge, whereas only oligomers occurred on the surface of high-charge Lap nanoparticles [217]. Another example is radical formation from the cationic dye safranin and its involvement in radical polymerization [218]. The photoinduced electron transfer between different organic dye molecules can be potentially applied in organic solar cells. Such reactions were reported between pyronine and Sb^V-porphyrine dye in hybrid films with Sap [219] or between $[Ru(2,2\text{-bipy})_2]^{2+}$ and methylviologen [220].

18.6 Applications in Research and Industry

18.6.1 Sensors

Numerous hybrid materials are based on organic molecules with sensing properties, which can be applied in various branches of analytical chemistry. They include sensors for pH, solvents, photochemical, and redox properties. The involvement of molecular probes and sensors in hybrid systems offers various advantages. They are relatively easy to prepare and the dye properties can be slightly tuned via the effect of host particles. Hybrid materials often provide improved stability and thermal resistance of the molecular probes. The photoactive molecules anchored on nanoparticles can be manipulated in similar ways, as pure nanoparticle systems, which can be easier than isolating or manipulating dye molecules in solutions. For example, hybrid colloids can undergo cyclic flocculation/peptization, could be isolated or purified by filtration, centrifugation, or dialysis. Layered particles can be incorporated into multicomponent films with well-defined molecular layers, such as LB films and LbL assemblies. MB and other phenothiazine dyes are well-known redox indicators changing to their colorless (leuco) form under reductive conditions. Electrochemistry of MB in the hybrid films with Mmt has been studied in detail [221]. MB performs in a similar way as in solutions. Furthermore, the electrochemistry of intercalated MB cations retains similar parameters at variable pH [222]. There are several examples of using MB as a sensor: The electrodes or sensors based on MB intercalated in layered compounds were developed for the analysis of ascorbic acid in commercial samples [223]. An MB hybrid with barium phosphate was used for the detection of the reduced form of nicotinamide adenine dinucleotide, NADH [224]. Sap modified with cationic surfactant and intercalated with the mixture of MB and reducing agent (either ascorbic acid or sugar) exhibited the properties of a sensitive O_2 sensor under anoxic conditions (<0.1% O_2) [225]. An amperometric biosensor using similar phenothiazine dye, azure B, intercalated in Lap was used for the detection of phenolic compounds. The dye acted as an electron shuttle with polyphenol oxidase reaching the detection limits in the range of nM concentrations [226]. Also other types of dyes were used as probes and sensors performing on various chemical reactions and phenomena. An interesting example is the solvatochromic properties of intercalated porphyrin dyes [101] (see Sect. 18.5.4). Another example is the detection of methanol, a highly toxic substance, which is very difficult to differentiate from other alcohols. It could be selectively detected by a composite film sensor prepared from oxoporphyrinogen and LDH [227]. Another example is sensing permanent water hardness based on FRET between two laser dyes, acriflavine and Rh B. The sensitivity was significantly increased when the dyes were incorporated in a Lap film [228]. The fluorescence quenching of photosensitizers with O_2 is another phenomenon which has been frequently applied in oxygen sensing [110]. The hybrid materials for multianalyte detection have not been significantly developed yet. In particular LbL assembly formation would be highly suitable for this purpose. Relatively new

applications use dye molecules as *in situ* probes of the processes occurring in the manufacture of polymers and their nanocomposites. Mmt modified with surfactants was doped with various fluorescent dyes for the real-time monitoring of polymer intercalation during nanocomposite processing [229]. In a similar study, Nile blue probe was used to monitor the compounding of nylon nanocomposites. The hybrid precursor was inactive due to the formation of dye aggregates, and luminescence appeared with the exfoliation of the layered particles in the polymer phase [230]. In another work, dye sensors were also used to inspect the morphology of polypropylene nanocomposites [231]. Dyes can also be used as *in situ* sensors for detecting the processes in colloids, to monitor transport in subsoils and aquifers [232].

18.6.2 Hybrids with Natural Dyes

Natural dyes have found their applications in various industrial fields. They are easily available, mostly at an affordable price, harmless enough to be used as food industry additives, in medicine or in cosmetics. Some natural dyes exhibit very interesting properties, such as biological activity, photosensitization, radical scavengers, luminescence, etc. There are several interesting examples of hybrid systems with natural dyes. Phycoerythrin, a natural pigment extracted from seaweed, was used for the synthesis of hybrid materials with Hec and Mmt. Bright fluorescence and higher stability against bleaching were achieved for the hybrid materials [51]. New hybrid materials were synthesized using a series of LDH samples and the natural pigment chlorophyll a. The extent of dye adsorption and the stability of the hybrid pigments depended on the type of inorganic host. The hybrid materials were more stable if LDH of Mg/Al-type were used, while catalytic decomposition occurred on the surface of Ni/Al-type LDH [233]. Low stability of carotenoids under irradiation limits their broader application in industry. An improvement in their stability was reported for beta-carotene and annatto dye intercalated in LDH. The host material had to be premodified with anionic surfactants to match the lipophilic properties of these dyes [194]. An improvement in thermal stability was reported for the hybrids of anthocyanins extracted from the acai fruit *Euterpe oleracea.* These dyes intercalated in Mmt or Sap exhibited the properties of efficient radical scavengers [234]. Nanohybrids with edible dyes used in the food industry were also investigated [235]. Natural red cabbage dye was used in electrodes combining Mmt and TiO_2 particles and tested in *natural dye solar cells* [236]. Abiogenic flavin and riboflavin-type chromophores prepared via the thermolysis of amino acid mixtures were adsorbed onto the particles of LSil. In this type of dyes, the adsorption significantly reduced their photosensitization properties [237]. Intercalation of the luminescent alkaloid berberine in Sap, altered its optical properties but did not reduce its photoactivity [151].

18.6.3 Hybrids Used in Biology, Medicine, and Agriculture

There is a limited number of hybrid systems applied in biology or medicine. Active dyes in the hybrid materials can actively participate in the interaction with living cells or play the role of biocides and photosensitizers. In some cases, antimicrobial properties can be reduced by the incorporation of active species into the hybrid material. An example is cationic p-phenylene ethynylenes intercalated in Lap [83]. On the other hand, the antimicrobial properties of MB adsorbed on Mmt colloid particles were significantly improved. The hybrid colloids were efficient against the sporulation of *Aspergilus niger* and *Penicillium sp.*, reduced the growth of the bacteria *Escherichia coli* and *Streptococus aureus*, and the yeast *Candida albicans*. The role of LSil particles was most likely to mediate the interaction between the microorganism cells and the photoactive MB [205, 238].

Staining is a technique using organic dyes to enhance contrast and highlight structures in microscopic images. In a few cases hybrid nanomaterials have been used for this purpose. The hybrids composed from quaternary tetraphenylethene probe intercalated in layered α-zirconium phosphate was developed as an effective fluorescence label for HeLa cells [239]. In another study, LDH nanoparticles were used as carriers to transport various organic biologically active substances to specific targets. In order to control their distribution, a near-infrared fluorescent probe (Cy5.5) was also incorporated. The functionalized particles acted as highly efficient contrast agents, since Cy5.5 probe molecules were stabilized by layered particles [240]. Nile red is a polarity probe, which is almost insoluble and non-emissive in water. It was stabilized and became photoactive in the hybrids with Lap. The hybrid materials have potential as optical probes for tumor imaging [90].

There are numerous examples of applying of dye/LSil hybrid systems in the stabilization of photolabile pesticides. The mechanism of the stabilization was assigned to FRET (see Sect. 18.5.4). The dye molecules playing the role of EA were carefully selected to match the energies of the excited states of the photolabile pesticide. Examples are bioresmethrin in Mmt co-adsorbed with cationic dye, methyl green [191], insecticide tetrahydro-2-(nitromethylene)-2H-1,3-thiazine with acriflavine [191] or 3,6-diamino-10-methylacridinium [241], microbial insecticides, such as the *Bacillus thuringiensis* toxin with various types of chromophores [191], insecticide tetrahydro-2-(nitromethylene)-2H-1,3-thiazine with cationic dye 3,6-diamino-10-methylacridinium [241], insecticide quinalphos with crystal violet [242], etc. In some cases other phenomena also played roles. For example, the steric stabilization of organic molecules on the particle surface, or photoquenching by Fe^{III} occurring in the matrix of some LSil [191].

18.6.4 Polymer Nanocomposites and Other Applications

Photofunctional materials based on industrial polymers can be prepared by the chemical modificiation of polymers with photoactive groups or directly during polymerization by incorporating the chromophoric units in polymer chains. The strategy via polymer nanocomposites is another, alternative way. Nanoparticles dispersed in the polymer matrix can play the role of carriers of photoactive dye molecules. Inorganic layered nanomaterials are not compatible with the hydrophobic nature of most industrial polymers, and their chemical premodification is mostly required. The most common way is based on modification with ionic surfactants. The organically modified layered particles are excellent sorbents forming stable colloids in organic solvents. Their complexes with organic dyes often exhibit high photoactivity [39]. The organically modified layered materials with adsorbed organic dyes are suitable precursors for polymer nanocomposites. Processing the polymer composite often requires an enhanced temperature and thermal stability of the hybrid precursors. There are a few works reporting an improvement in dye thermal stability in hybrid materials (see Sect. 18.5.5). One example is a nanopigment based on Basic Blue 41 intercalated in Na^+-Mmt [243]. The nanocomposites based on MB, Mmt, and poly(ethylene vinyl acetate) exhibited superior optical as well as mechanical properties [244]. Similar nanocomposites were reported in other studies [245, 246]. The superior properties of organically modified LSil were confirmed in the studies using laser dyes. An example is Rh B/organically modified Mmt composites with polypropylene [247]. Complexes of Rh 6G and nonmodified Mmt were also incorporated into polyethylene [248]. UV-exposure tests on colored Rh B/Mmt/polypropylene composites showed significant improvements in dye photostability [201]. LDH and hydroxide nanosheets bearing organic dyes were also applied: Layered $Zn(OH)_2$ with anionic orange azo dyes (methyl orange or methyl orange II) were used as the fillers for high-density polyethylene [249]. Composites of poly(vinyl alcohol) containing LDH particles with adsorbed anionic azo dyes were also investigated [250, 251]. Nanocomposites exhibiting nonlinear optical properties were prepared from dibenzilidene acetone-type chromophores intercalated in LSil. Active J-aggregates were preserved in the composite with poly(propylene) [176]. Nanoparticles can significantly affect the optical properties of polymers with chromophoric groups. LSil nanocomposites with poly(styrene) carrying fluorescent terfluorene side chains were used for the fabrication of transparent films with a controlled morphology. The films exhibited the properties of efficient emitters which has potential for their application in light-emitting devices [252]. Polyurethane with azo dye moieties was used for the preparation of nanocomposites containing various amounts of organically modified Mmt. Mmt layers were completely exfoliated in the polymer matrix, and the nanocomposites exhibited some mechanical properties that were superior to the pure polymer [253].

Besides the polymer industry, there are further technical branches of potential hybrid material applications which are worth mentioning. Some hybrid systems

have been tested as an alternative approach for dyeing industrial textiles [254, 255]. Another example are pigments applied for thermal dye transfer printing. The studied systems included organically modified LSil with fluoran [256], Rh 6G [257], and other dyes [258]. The adsorption improved dye stability in some cases [259]. The hybrids with triphenylmethane dyes were investigated for their application in commercial carbonless copying paper [204]. Fluoran dye intercalated in organically modified LSil exhibited the properties of a reversible color change via electrochemical activation. Such materials could be used in rewritable recording media controlled by electrostatic potential [260]. Rather chemical properties of MB immobilized in LSil was used for an efficient extraction of Hg^{2+} from waste waters. The sorbent could be quantitatively recovered by a controlled Hg^{2+}release via treatment with NH_3 [261].

18.7 Conclusions

Knowledge on hybrid materials has increased significantly over the last few decades. Numerous applications in the field have emerged by the combination of various constituents including molecules, polymeric substances, nanoparticles, compounds of biological origin into a single material. The combination of various substances at a molecular level provides extraordinary properties and various functionalities, and quantitatively an almost infinite number of new material types. With the development of novel fields in nanosciences, there are new demands in terms of material properties. The development of hybrids of layered nanoparticles with organic dyes has also spread into new areas of materials science. Interest in old types of materials has decreased and the emphasis is aimed on bioactive, biocompatible, electronic, optical, optoelectronic, and magnetic materials. These novel hybrid materials could be used in biochemistry, medicine, environmental sciences, electronics, optics, etc. The rapid development of these hybrid materials is being accelerated by modern research methods, such as high resolution microscopy or single-molecule spectroscopy methods. Modern technologies have developed new techniques for precisely organizing nanoscale building blocks and other constituents and to precisely tuning the material's structure to achieve the formation of the desired complex and multifunctional systems. Modern physicochemical methods combined with the latest knowledge are opening up new prospects in chemistry, such as the field of molecular and nanomaterial engineering for configuring novel material designs.

Acknowledgments This work was supported by the Slovak Research and Development Agency under the contract No. APVV-0291-11, APVV-15-0347. Support from Grant Agency VEGA (1/0278/16) is also acknowledged.

References

1. Zhang Y, Fan L, Chen H, Zhang J, Zhang Y, Wang A (2015) Learning from ancient Maya: preparation of stable palygorskite/methylene blue@SiO2 Maya Blue-like pigment. Microporous Mesoporous Mater 211:124–133. doi:10.1016/j.micromeso.2015.03.002
2. Giustetto R, Vitillo JG, Corazzari I, Turci F (2014) Evolution and reversibility of host/guest interactions with temperature changes in a Methyl Red@Palygorskite polyfunctional hybrid nanocomposite. J Phys Chem C 118(33):19322–19337. doi:10.1021/jp4091238
3. Domenech-Carbo A, Domenech-Carbo MT, Osete-Cortina L, Valle-Algarra FM, Buti D (2014) Isomerization and redox tuning in 'Maya yellow' hybrids from flavonoid dyes plus palygorskite and kaolinite clays. Microporous Mesoporous Mater 194:135–145. doi:10.1016/j.micromeso.2014.03.046
4. Ogawa M, Kuroda K (1995) Photofunctions of intercalation compounds. Chem Rev 95 (2):399–438. doi:10.1021/cr00034a005
5. Schulz-Ekloff G, Wohrle D, van Duffel B, Schoonheydt RA (2002) Chromophores in porous silicas and minerals: preparation and optical properties. Microporous Mesoporous Mater 51 (2):91–138
6. Lezhnina MM, Kynast UH (2010) Optical properties of matrix confined species. Opt Mater 33(1):4–13. doi:10.1016/j.optmat.2010.07.005
7. Latterini L, Nocchetti M, Aloisi GG, Costantino U, Elisei F (2007) Organized chromophores in layered inorganic matrices. Inorg Chim Acta 360(3):728–740. doi:10.1016/j.ica.2006.07.048
8. Demel J, Lang K (2012) Layered hydroxide-porphyrin hybrid materials: synthesis, structure, and properties. Eur J Inorg Chem 32:5154–5164. doi:10.1002/ejic.201200400
9. Takagi S, Eguchi M, Tryk DA, Inoue H (2006) Porphyrin photochemistry in inorganic/organic hybrid materials: clays, layered semiconductors, nanotubes, and mesoporous materials. J Photochem Photobiol, C 7(2–3):104–126. doi:10.1016/j.jphotochemrev.2006.04.002
10. Liu P, Zhang L (2007) Adsorption of dyes from aqueous solutions or suspensions with clay nano-adsorbents. Sep Purif Technol 58 (1):32–39. doi:http://dx.doi.org/10.1016/j.seppur.2007.07.007
11. Zhou CH, Shen ZF, Liu LH, Liu SM (2011) Preparation and functionality of clay-containing films. J Mater Chem 21(39):15132–15153
12. Bujdák J (2006) Effect of the layer charge of clay minerals on optical properties of organic dyes. A review. Appl Clay Sci 34(1–4):58–73. doi:10.1016/j.clay.2006.02.011
13. Schoonheydt RA (2002) Smectite-type clay minerals as nanomaterials. Clays Clay Miner 50(4):411–420
14. Okada T, Sohmiya M, Ogawa M (2015) Photochromic intercalation compounds. Struct Bond 166:177–211. doi:10.1007/978-3-319-16991-0-5
15. Arbeloa FL, Martinez V, Arbeloa T, Arbeloa IL (2010) Fluorescence anisotropy to study the preferential orientation of fluorophores in ordered bi-dimensional systems: rhodamine 6G/Laponite layered films. In: Geddes CD (ed) Reviews in fluorescence 2008, vol 5. Reviews in fluorescence. Kluwer Academic/Plenum Publ, New York, pp 1–35. doi:10.1007/978-1-4419-1260-2_1
16. Neumann MG, Gessner F (2002) Adsorption of Dyes on Clay Surfaces. In: Hubbard AT (ed) Encyclopedia of surface and colloid science, vol 1. Marcel Dekker A.G, New York, pp 307–320
17. Yariv S (2002) Staining of clay minerals and visible absorption spectroscopy of dye-clay complexes. In: Yariv S, Cross H (eds) Organo-clay complexes and interactions. Marcel Dekker, New York, pp 463–566
18. Lagaly G, Ogawa M, Dekany I (2013) Clay mineral-organic interactions. In: Bergaya F, Lagaly G (eds) Handbook of clay science, 2nd edn. Elsevier, Amsterdam, pp 435–505
19. Stewart TA, Nyman M, Deboer MP (2011) Delaminated titanate and peroxotitanate photocatalysts. Appl Catal B 105(1–2):69–76. doi:10.1016/j.apcatb.2011.03.036

20. Nakato T, Inoue S, Hiraragi Y, Sugawara J, Mouri E, Aritani H (2014) Decomposition of a cyanine dye in binary nanosheet colloids of photocatalytically active niobate and inert clay. J Mater Sci 49(2):915–922. doi:10.1007/s10853-013-7777-8
21. Miyamoto N, Nakato T (2003) Liquid crystalline colloidal system obtained by mixing niobate and aluminosilicate nanosheets: a spectroscopic study using a probe dye. Langmuir 19(19):8057–8064. doi:10.1021/la0268449
22. Nakato T, Yamashita Y, Kuroda K (2006) Mesophase of colloidally dispersed nanosheets prepared by exfoliation of layered titanate and niobate. Thin Solid Films 495(1–2):24–28. doi:10.1016/j.tsf.2005.08.301
23. Rytwo G, Nir S, Margulies L (1995) Interactions of monovalent organic cations with montmorillonite—adsorption studies and model-calculations. Soil Sci Soc Am J 59(2):554–564
24. Chen Y (2015) Nanotubes and nanosheets: functionalization and applications of boron nitride and other nanomaterials. CRC Press, New York
25. Rives V (2001) Layered double hydroxides: present and future. Nova Science Publishers, New York
26. Auerbach SM, Carrado KA, Dutta PK (2004) Handbook of layered materials. CRC Press, New York
27. Bujdák J, Komadel P (1997) Interaction of methylene blue with reduced charge montmorillonite. J Phys Chem B 101(44):9065–9068
28. Bujdák J, Janek M, Madejová J, Komadel P (1998) Influence of the layer charge density of smectites on the interaction with methylene blue. J Chem Soc, Faraday Trans 94(23):3487–3492
29. Bujdák J, Iyi N, Kaneko Y, Czímerová A, Sasai R (2003) Molecular arrangement of rhodamine 6G cations in the films of layered silicates: the effect of the layer charge. Phys Chem Chem Phys 5(20):4680–4685. doi:10.1039/b305699f
30. Bujdák J, Iyi N (2006) Molecular aggregation of rhodamine dyes in dispersions of layered silicates: influence of dye molecular structure and silicate properties. J Phys Chem B 110 (5):2180–2186. doi:10.1021/jp0553378
31. Chen GM, Iyi NB, Sasai R, Fujita T, Kitamura K (2002) Intercalation of rhodamine 6G and oxazine 4 into oriented clay films and their alignment. J Mater Res 17(5):1035–1040
32. Iyi N, Sasai R, Fujita T, Deguchi T, Sota T, Arbeloa FL, Kitamura K (2002) Orientation and aggregation of cationic laser dyes in a fluoromica: polarized spectrometry studies. Appl Clay Sci 22(3):125–136
33. Bujdák J, Iyi N (2006) Spectral and structural characteristics of oxazine 4/hexadecyltrimethylammonium montmorillonite films. Chem Mater 18(10):2618–2624. doi:10.1021/cm052715c
34. Miyamoto N, Nakato T (2002) Liquid crystalline nature of K4Nb6O17 nanosheet sols and their macroscopic alignment. Adv Mater 14(18):1267–1270
35. Hibino T, Jones W (2001) New approach to the delamination of layered double hydroxides. J Mater Chem 11(5):1321–1323. doi:10.1039/b101135i
36. Li L, Ma RZ, Ebina Y, Iyi N, Sasaki T (2005) Positively charged nanosheets derived via total delamination of layered double hydroxides. Chem Mater 17(17):4386–4391. doi:10.1021/cm0510460
37. Iyi N, Yamada H (2012) Efficient decarbonation of carbonate-type layered double hydroxide (CO32-LDH) by ammonium salts in alcohol medium. Appl Clay Sci 65–66:121–127. doi:10.1016/j.clay.2012.05.001
38. Iyi N, Yamada H, Sasaki T (2011) Deintercalation of carbonate ions from carbonate-type layered double hydroxides (LDHs) using acid-alcohol mixed solutions. Appl Clay Sci 54 (2):132–137. doi:10.1016/j.clay.2011.07.017
39. Bujdák J, Iyi N (2012) Highly fluorescent colloids based on rhodamine 6G, modified layered silicate, and organic solvent. J Colloid Interface Sci 388(1):15–20. doi:10.1016/j.jcis.2012.08.020
40. Eyama T, Yogo Y, Fujimura T, Tsukamoto T, Masui D, Shimada T, Tachibana H, Inoue H, Takagi S (2012) Adsorption and stacking behaviour of zwitterionic porphyrin on the clay surface. Clay Miner 47(2):243–250. doi:10.1180/claymin.2012.047.2.07

41. Luo ZX, Gao ML, Ye YG, Yang SF (2015) Modification of reduced-charge montmorillonites by a series of Gemini surfactants: characterization and application in methyl orange removal. Appl Surf Sci 324:807–816. doi:10.1016/j.apsusc.2014.11.043
42. Hata H, Kobayashi Y, Mallouk TE (2007) Encapsulation of anionic dye molecules by a swelling fluoromica through intercalation of cationic polyelectrolytes. Chem Mater 19(1):79–87. doi:10.1021/cm061908c
43. Gunister E, Bozkurt AM, Catalgil-Giz H (2013) Poly (diallyldimethylammoniumchloride)/sodium-montmorillonite composite; structure, and adsorption properties. J Appl Polym Sci 129(3):1232–1237. doi:10.1002/app.38792
44. Hao YF, Yan LG, Yu HQ, Yang K, Yu SJ, Shan RR, Du B (2014) Comparative study on adsorption of basic and acid dyes by hydroxy-aluminum pillared bentonite. J Mol Liq 199:202–207. doi:10.1016/j.molliq.2014.09.005
45. Qin ZH, Yuan P, Yang SQ, Liu D, He HP, Zhu JX (2014) Silylation of Al-13-intercalated montmorillonite with trimethylchlorosilane and their adsorption for Orange II. Appl Clay Sci 99:229–236. doi:10.1016/j.clay.2014.06.038
46. Tireli AA, Marcos FCF, Oliveira LF, Guimaraes ID, Guerreiro MC, Silva JP (2014) Influence of magnetic field on the adsorption of organic compound by clays modified with iron. Appl Clay Sci 97–98:1–7. doi:10.1016/j.clay.2014.05.014
47. Wlodarczyk P, Komarneni S, Roy R, White WB (1996) Enhanced fluorescence of coumarin laser dye in the restricted geometry of a porous nanocomposite. J Mater Chem 6(12):1967–1969
48. Felbeck T, Mundinger S, Lezhnina MM, Staniford M, Resch-Genger U, Kynast UH (2015) Multifold fluorescence enhancement in nanoscopic fluorophore-clay hybrids in transparent aqueous media. Chem Eur J 21(20):7582–7587. doi:10.1002/chem.201406416
49. Giustetto R, Seenivasan K, Bonino F, Ricchiardi G, Bordiga S, Chierotti MR, Gobetto R (2011) Host/guest interactions in a sepiolite-based maya blue pigment: a spectroscopic study. J Phys Chem C 115(34):16764–16776. doi:10.1021/jp203270c
50. Zhang YJ, Fan L, Zhang JP, Wang AQ (2015) Water-dispersible and stable fluorescent Maya Blue-like pigments. RSC Adv 5(44):35010–35016. doi:10.1039/c5ra01863c
51. Lin YH, Hori Y, Hoshino S, Miyazawa C, Kohno Y, Shibata M (2014) Fluorescent colored material made of clay mineral and phycoerythrin pigment derived from seaweed. Dyes Pigm 100:97–103. doi:10.1016/j.dyepig.2013.08.022
52. Lezhnina MM, Grewe T, Stoehr H, Kynast U (2012) Laponite blue: dissolving the insoluble. Angew Chem Int Ed 51(42):10652–10655. doi:10.1002/anie.201203236
53. Carrado KA, Forman JE, Botto RE, Winans RE (1993) Incorporation of phthalocyanines by cationic and anionic clays via ion-exchange and direct synthesis. Chem Mater 5(4):472–478
54. Fujii K, Hayashi S (eds) (2003) Syntheses of smectite-analogue/coumarin composites. 2001—a Clay Odyssey. Elsevier Science B.V., Amsterdam, Netherlands
55. Xue AL, Zhou SY, Zhao YJ, Lu XP, Han PF (2010) Adsorption of reactive dyes from aqueous solution by silylated palygorskite. Appl Clay Sci 48(4):638–640. doi:10.1016/j.clay.2010.03.011
56. Fujii K, Kuroda T, Sakoda K, Iyi N (2011) Fluorescence resonance energy transfer and arrangements of fluorophores in integrated coumarin/cyanine systems within solid-state two-dimensional nanospace. J Photochem Photobiol, A 225(1):125–134. doi:10.1016/j.jphotochem.2011.10.009
57. Fujii K, Iyi N, Sasai R, Hayashi S (2008) Preparation of a novel luminous heterogeneous system: rhodamine/coumarin/phyllosilicate hybrid and blue shift in fluorescence emission. Chem Mater 20(9):2994–3002. doi:10.1021/cm0716452
58. Bujdák J, Danko M, Chorvát D Jr, Czímerová A, Sýkora J, Lang K (2012) Selective modification of layered silicate nanoparticle edges with fluorophores. Appl Clay Sci 65–66:152–157. doi:10.1016/j.clay.2012.04.029
59. Al Bakain RZ, Al-Degs YS, Issa AA, Jawad SA, Abu Safieh KA, Al-Ghouti MA (2014) Activation of kaolin with minimum solvent consumption by microwave heating. Clay Miner 49(5):667–681. doi:10.1180/claymin.2014.049.5.04

60. Sas S, Danko M, Lang K, Bujdák J (2015) Photoactive hybrid material based on kaolinite intercalated with a reactive fluorescent silane. Appl Clay Sci 108:208–214. doi:10.1016/j.clay.2015.02.031
61. Okada T, Yoshido S, Miura H, Yamakami T, Sakai T, Mishima S (2012) Swellable microsphere of a layered silicate produced by using monodispersed silica particles. J Phys Chem C 116(41):21864–21869. doi:10.1021/jp307108t
62. Suzuki Y, Hirakawa S, Sakamoto Y, Kawamata J, Kamada K, Ohta K (2008) Hybrid films consisting of a clay and a diacetylenic two-photon absorptive dye. Clays Clay Miner 56(5):487–493. doi:10.1346/ccmn.2008.0560501
63. Shil A, Hussain SA, Bhattacharjee D (2015) Adsorption of a water soluble cationic dye into a cationic Langmuir monolayer. J Phys Chem Solids 80:98–104. doi:10.1016/j.jpcs.2015.01.005
64. Ras RHA, Nemeth J, Johnston CT, DiMasi E, Dekany I, Schoonheydt RA (2004) Hybrid Langmuir-Blodgett monolayers containing clay minerals: effect of clay concentration and surface charge density on the film formation. Phys Chem Chem Phys 6(16):4174–4184. doi:10.1039/b405862c
65. Ras RHA, Nemeth J, Johnston CT, Dekany I, Schoonheydt RA (2004) Orientation and conformation of octadecyl rhodamine B in hybrid Langmuir-Blodgett monolayers containing clay minerals. Phys Chem Chem Phys 6(23):5347–5352. doi:10.1039/b411339j
66. Bhattacharjee J, Hussain SA, Bhattacharjee D (2013) Control of H-dimer formation of acridine orange using nano clay platelets. Spectrochim Acta A Mol Biomol Spectrosc 116:148–153. doi:10.1016/j.saa.2013.07.018
67. Bujdák J (2014) Layer-by-layer assemblies composed of polycationic electrolyte, organic dyes, and layered silicates. J Phys Chem C 118(13):7152–7162. doi:10.1021/jp411155x
68. Place I, Penner TL, McBranch DW, Whitten DG (2003) Layered nanocomposites of aggregated dyes and inorganic scaffolding. J Phys Chem A 107(18):3169–3177. doi:10.1021/jp026048b
69. Leone G, Giovanella U, Bertini F, Porzio W, Meinardi F, Botta C, Ricci G (2013) Poly (styrene)-graft-/rhodamine 6G-fluoromica hybrids: synthesis, characterization and photophysical properties. J Mater Chem C 1(7):1450–1460. doi:10.1039/c2tc00533f
70. Nakamura T, Ogawa M (2013) Adsorption of cationic dyes within spherical particles of poly (N-isopropylacrylamide) hydrogel containing smectite. Appl Clay Sci 83–84:469–473. doi:10.1016/j.clay.2013.05.005
71. Olivero F, Carniato F, Bisio C, Marchese L (2012) A novel stable and efficient light-emitting solid based on saponite and luminescent POSS. J Mater Chem 22(48):25254–25261. doi:10.1039/c2jm34230h
72. Suchithra PS, Vazhayal L, Mohamed AP, Ananthakumar S (2012) Mesoporous organic-inorganic hybrid aerogels through ultrasonic assisted sol-gel intercalation of silica-PEG in bentonite for effective removal of dyes, volatile organic pollutants and petroleum products from aqueous solution. Chem Eng J 200:589–600. doi:10.1016/j.cej.2012.06.083
73. Zhang YX, Hao XD, Kuang M, Zhao H, Wen ZQ (2013) Preparation, characterization and dye adsorption of Au nanoparticles/ZnAl layered double oxides nanocomposites. Appl Surf Sci 283:505–512. doi:10.1016/j.apsusc.2013.06.136
74. Kobayashi T (2012) J-Aggregates, vol 2. World Scientific, Signapore
75. Bergmann K, O'Konski CT (1963) A spectroscopic study of methylene blue monomer, dimer, and complexes with montmorillonite. J Phys Chem 67(10):2169–2177
76. Bujdák J, Iyi N, Fujita T (2002) The aggregation of methylene blue in montmorillonite dispersions. Clay Miner 37(1):121–133. doi:10.1180/0009855023710022
77. Breen C, Loughlin H (1994) The competitive adsorption of methylene-blue on to Na-montmorillonite from binary-solution with N-alkylytrimethylammonium surfactants. Clay Miner 29(5):775–783
78. Gessner F, Schmitt CC, Neumann MG (1994) Time-dependent spectrophotometric study of the interaction of basic-dyes with clays. 1. Methylene-blue and neutral red on Montmorrillonite and Hectorite. Langmuir 10(10):3749–3753

79. Lofaj M, Valent I, Bujdák J (2013) Mechanism of rhodamine 6G molecular aggregation in montmorillonite colloid. Cent Eur J Chem 11(10):1606–1619. doi:10.2478/s11532-013-0289-1
80. Arbeloa FL, Martinez VM, Arbeloa T, Arbeloa IL (2007) Photoresponse and anisotropy of rhodamine dye intercalated in ordered clay layered films. J Photochem Photobiol, C 8:85–108. doi:10.1016/j.jphotochemrev.2007.03.003
81. Tsurumachi N, Okamoto H, Ishii K, Kohkami H, Nakanishi S, Ishii T, Takahashi N, Dou CS, Wen PH, Feng Q (2012) Formation of aggregates in nanohybrid material of dye molecules-titanate nanosheets. J Photochem Photobiol, A 243:1–6. doi:10.1016/j.jphotochem.2012.05.022
82. Tsukamoto T, Shimada T, Takagi S (2013) Photochemical properties of mono-, Tr-, and penta-cationic antimony(V) metalloporphyrin derivatives on a clay layer surface. J Phys Chem A 117(33):7823–7832. doi:10.1021/jp405767s
83. Hill EH, Zhang Y, Whitten DG (2015) Aggregation of cationic p-phenylene ethynylenes on Laponite clay in aqueous dispersions and solid films. J Colloid Interface Sci 449:347–356. doi:10.1016/j.jcis.2014.12.006
84. Ishida Y, Shimada T, Tachibana H, Inoue H, Takagi S (2013) Regulation of the collisional self-quenching of fluorescence in clay/porphyrin complex by strong host-guest interaction. J Phys Chem A 116(49):12065–12072. doi:10.1021/jp309502j
85. Ishida Y, Shimada T, Takagi S (2014) Surface-fixation induced emission of porphyrazine dye by a complexation with inorganic nanosheets. J Phys Chem C 118(35):20466–20471. doi:10.1021/jp506766t
86. Ferreira AUC, Poli AL, Gessner F, Neumann MG, Cavalheiro CCS (2013) Interaction of Auramine O with montmorillonite clays. J Lumin 136:63–67. doi:10.1016/j.jlumin.2012.11.022
87. Valandro SR, Poli AL, Neumann MG, Schmitt CC (2015) Photophysics of Auramine O adsorbed on solid clays. J Lumin 161:209–213. doi:10.1016/j.jlumin.2015.01.023
88. Sun ZZ, Wang J, Wei HY, Wang GQ, Jian Y, Luo SZ, Zhou ZJ (2014) Spectroscopic investigation of a synthetic cyanine amine derivative upon various scaffolds. Anal Lett 47 (16):2722–2730. doi:10.1080/00032719.2014.919505
89. Chakraborty S, Debnath P, Dey D, Bhattacharjee D, Hussain SA (2014) Formation of fluorescent H-aggregates of a cyanine dye in ultrathin film and its effect on energy transfer. J Photochem Photobiol, A 293:57–64. doi:10.1016/j.jphotochem.2014.07.018
90. Felbeck T, Behnke T, Hoffmann K, Grabolle M, Lezhnina MM, Kynast UH, Resch-Genger U (2013) Nile-red-nanoclay hybrids: red emissive optical probes for use in aqueous dispersion. Langmuir 29(36):11489–11497. doi:10.1021/la402165q
91. Costa AL, Gomes AC, Pillinger M, Gonçalves IS, De melo JSS (2015) An indigo carmine-based hybrid nanocomposite with supramolecular control of dye aggregation and photobehavior. Chem Eur J 21 (34):12069–12078. doi:10.1002/chem.201501344
92. Bujdák J, Iyi N (2002) Visible spectroscopy of cationic dyes in dispersions with reduced-charge montmorillonites. Clays Clay Miner 50(4):446–454
93. Bujdák J, Iyi N, Sasai R (2004) Spectral properties, formation of dye molecular aggregates, and reactions in rhodamine 6G/layered silicate dispersions. J Phys Chem B 108(14):4470–4477. doi:10.1021/jp037607x
94. Cione APP, Schmitt CC, Neumann MG, Gessner F (2000) The effect of added salt on the aggregation of clay particles. J Colloid Interface Sci 226(2):205–209
95. Czímerová A, Bujdák J, Gáplovský A (2004) The aggregation of thionine and methylene blue dye in smectite dispersion. Colloids Surf A 243(1–3):89–96. doi:10.1016/j.solsurfa.2004.05.002
96. Czímerová A, Bujdák J, Dohrmann R (2006) Traditional and novel methods for estimating the layer charge of smectites. Appl Clay Sci 34(1–4):2–13. doi:10.1016/j.clay.2006.02.008
97. Bujdák J, Janek M, Madejová J, Komadel P (2001) Methylene blue interactions with reduced-charge smectites. Clays Clay Miner 49(3):244–254

98. Bujdák J, Iyi N, Hrobáriková J, Fujita T (2002) Aggregation and decomposition of a pseudoisocyanine dye in dispersions of layered silicates. J Colloid Interface Sci 247(2):494–503. doi:10.1006/jcis.2001.8140
99. Ishida Y, Masui D, Tachibana H, Inoue H, Shimada T, Takagi S (2012) Controlling the microadsorption structure of porphyrin dye assembly on clay surfaces using the "size-matching rule" for constructing an efficient energy transfer system. ACS Appl Mater Interfaces 4(2):811–816. doi:10.1021/am201465a
100. Fujimura T, Shimada T, Hamatani S, Onodera S, Sasai R, Inoue H, Takagi S (2013) High density intercalation of porphyrin into transparent clay membrane without aggregation. Langmuir 29(16):5060–5065. doi:10.1021/la4003737
101. Takagi S, Shimada T, Ishida Y, Fujimura T, Masui D, Tachibana H, Eguchi M, Inoue H (2013) Size-matching effect on inorganic nanosheets: control of distance, alignment, and orientation of molecular adsorption as a bottom-up methodology for nanomaterials. Langmuir 29(7):2108–2119. doi:10.1021/la3034808
102. Chakraborty C, Dana K, Malik S (2011) Intercalation of perylenediimide dye into LDH clays: enhancement of photostability. J Phys Chem C 115(5):1996–2004. doi:10.1021/jp110486r
103. Tani S, Yamaki H, Sumiyoshi A, Suzuki Y, Hasegawa S, Yamazaki S, Kawamata J (2009) Enhanced photodegradation of organic dyes adsorbed on a clay. J Nanosci Nanotechnol 9 (1):658–661. doi:10.1166/jnn.2009.J081
104. Chernia Z, Gill D (1999) Flattening of TMPyP adsorbed on laponite. Evidence in observed and calculated UV-vis spectra. Langmuir 15(5):1625–1633
105. Miyamoto N, Kawai R, Kuroda K, Ogawa M (2000) Adsorption and aggregation of a cationic cyanine dye on layered clay minerals. Appl Clay Sci 16(3–4):161–170
106. Miyamoto N, Kuroda K, Ogawa M (2004) Exfoliation and film preparation of a layered titanate, $Na_2Ti_3O_7$, and intercalation of pseudoisocyanine dye. J Mater Chem 14(2):165–170. doi:10.1039/b308800f
107. Bujdák J, Iyi N (2008) Spectral properties and structure of the J-aggregates of pseudoisocyanine dye in layered silicate films. J Colloid Interface Sci 326(2):426–432. doi:10.1016/j.jcis.2008.06.036
108. Leone G, Giovanella U, Porzio W, Botta C, Ricci G (2011) In situ synthesis of fluorescent poly(norbornene)/oxazine-1 dye loaded fluoromica hybrids: supramolecular control over dye arrangement. J Mater Chem 21(34):12901–12909. doi:10.1039/c1jm11281c
109. Sasai R, Iyi N, Fujita TH, Takagi K, Itoh H (2003) Synthesis of rhodamine 6G/cationic surfactant/clay hybrid materials and its luminescent characterization. Chem Lett 32(6):550–551
110. Lang K, Kubat P, Mosinger J, Bujdak J, Hof M, Janda P, Sykora J, Iyi N (2008) Photoactive oriented films of layered double hydroxides. Phys Chem Chem Phys 10(30):4429–4434. doi:10.1039/b805081c
111. Sun ZY, Jin L, Shi WY, Wei M, Evans DG, Duan X (2011) Controllable photoluminescence properties of an anion-dye-intercalated layered double hydroxide by adjusting the confined environment. Langmuir 27(11):7113–7120. doi:10.1021/la200846j
112. Sasai R, Itoh T, Ohmori W, Itoh H, Kusunoki M (2009) Preparation and characterization of rhodamine 6G/Alkyltrimethylammonium/laponite hybrid solid materials with higher emission quantum yield. J Phys Chem C 113(1):415–421. doi:10.1021/jp805201n
113. Sasai R, Itoh T, Iyi N, Takagi K, Itoh H (2005) Preparation of hybrid organic/inorganic luminescent thin solid films with highly concentrated laser-dye cations. Chem Lett 34 (11):1490–1491. doi:10.1246/cl.2005.1490
114. Salleres S, Arbeloa FL, Martinez V, Corcostegui C, Arbeloa IL (2009) Effect of surfactant C12TMA molecules on the self-association of R6G dye in thin films of laponite clay. Mater Chem Phys 116(2–3):550–556. doi:10.1016/j.matchemphys.2009.04.030
115. Sasai R, Iyi N, Fujita T, Arbeloa FL, Martinez VM, Takagi K, Itoh H (2004) Luminescence properties of rhodamine 6G intercalated in surfactant/clay hybrid thin solid films. Langmuir 20(11):4715–4719. doi:10.1021/la049584z

116. Kaya M, Meral K, Onganer Y (2015) Molecular aggregates of Merocyanine 540 in aqueous suspensions containing natural and CTAB-modified bentonite. J Mol Struct 1083:101–105. doi:10.1016/j.molstruc.2014.11.046
117. Belušáková S, Lang K, Bujdák J (2015) Hybrid systems based on layered silicate and organic dyes for cascade energy transfer. J Phys Chem C 119:21784–21794. doi:10.1021/acs.jpcc.5b04982
118. Salleres S, Arbeloa FL, Martinez VM, Arbeloa T, Arbeloa IL (2010) On the arrangements of R6G molecules in organophilic C12TMA/lap clay films for low dye loadings. Langmuir 26 (2):930–937. doi:10.1021/la902414n
119. Konno S, Fujimura T, Otani Y, Shimada T, Inoue H, Takagi S (2014) Microstructures of the porphyrin/viologen mono layer on the clay surface: segregation or integration? J Phys Chem C 118(35):20504–20510. doi:10.1021/jp5076274
120. Sasai R, Iyi N, Kusumoto H (2011) Luminous change of rhodamine 3B incorporated into titanate nanosheet/decyltrimethylammonium hybrids under humid atmosphere. Bull Chem Soc Jpn 84(5):562–568. doi:10.1246/bcsj.20100343
121. Ishida Y, Kulasekharan R, Shimada T, Ramamurthy V, Takagi S (2014) Supramolecular-surface photochemistry: supramolecular assembly organized on a clay surface facilitates energy transfer between an encapsulated donor and a free acceptor. J Phys Chem C 118(19):10198–10203. doi:10.1021/jp502816j
122. Matejdes M, Czímerová A, Janek M (2015) Fluorescence tuning of 2D montmorillonite optically active layers with beta-cyclodextrine/dye supramolecular complexes. Appl Clay Sci 114:9–19. doi:10.1016/j.clay.2015.05.002
123. Yurekli K, Conley E, Krishnamoorti R (2005) Effect of laponite and a nonionic polymer on the absorption character of cationic dye solutions. Langmuir 21(13):5825–5830. doi:10.1021/la047540k
124. Vanamudan A, Pamidimukkala P (2015) Chitosan, nanoclay and chitosan-nanoclay composite as adsorbents for Rhodamine-6G and the resulting optical properties. Int J Biol Macromol 74:127–135. doi:10.1016/j.ijbiomac.2014.11.009
125. Czimerová A, Jankovič L, Madejová J, Čeklovský A (2013) Unique photoactive nanocomposites based on rhodamine 6G/polymer/montmorillonite hybrid systems. J Polym Sci, Part B: Polym Phys 51(23):1672–1679. doi:10.1002/polb.23382
126. Holzheu S, Hoffmann H (2002) Adsorption study of cationic dyes having a trimethylammonium anchor group on hectorite using electrooptic and spectroscopic methods. J Colloid Interface Sci 245(1):16–23. doi:10.1006/jcis.2001.7978
127. Bujdák J, Iyi N (2005) Molecular orientation of rhodamine dyes on surfaces of layered silicates. J Phys Chem B 109(10):4608–4615
128. Miyamoto N, Kuroda K, Ogawa M (2001) Uni-directional orientation of cyanine dye aggregates on a K4Nb6O17 single crystal: toward novel supramolecular assemblies with three-dimensional anisotropy. J Am Chem Soc 123(28):6949–6950. doi:10.1021/ja015541i
129. Hähner G, Marti A, Spencer ND, Caseri WR (1996) Orientation and electronic structure of methylene blue on mica: A near edge x-ray absorption fine structure spectroscopy study. J Chem Phys 104(19):7749–7757
130. Fischer D, Caseri WR, Hahner G (1998) Orientation and electronic structure of ion exchanged dye molecules on mica: an X-ray absorption study. J Colloid Interface Sci 198 (2):337–346
131. Wang HH, Han DX, Li N, Li KE (2005) Study on the intercalation and interlayer state of porphyrins into alpha-zirconium phosphate. J Incl Phenom Macrocycl Chem 52(3–4):247–252. doi:10.1007/s10847-004-7597-1
132. Čeklovský A, Bujdák J, Czímerová A, Iyi N (2007) Spectral study on the molecular orientation of a tetracationic porphyrin dye on the surface of layered silicates. Cent Eur J Phys 5(2):236–243. doi:10.2478/s11534-007-0010-0
133. Hayashi H, Hudson MJ (1995) Intercalation of the Copper(II) phthalocyanine Tetrasulfonate Anion ($CuPcTs^{4-}$) into basic Copper(II) salts. J Mater Chem 5(5):781–783. doi:10.1039/jm9950500781

134. Yan D, Lu J, Ma J, Wei M, Li S, Evans DG, Duan X (2011) Near-infrared absorption and polarized luminescent ultrathin films based on sulfonated cyanines and layered double hydroxide. J Phys Chem C 115(16):7939–7946. doi:10.1021/jp2002029
135. Windsor SA, Tinker MH (1999) Electro-fluorescence polarization studies of the interaction of fluorescent dyes with clay minerals in suspensions. Colloids Surf A 148(1–2):61–73
136. Salleres S, Arbeloa FL, Martinez VM, Arbeloa T, Arbeloa IL (2009) Improving the fluorescence polarization method to evaluate the orientation of fluorescent systems adsorbed in ordered layered materials. J Lumin 129(11):1336–1340. doi:10.1016/j.jlumin.2009.06.022
137. López Arbeloa F, Martínez Martínez V (2006) New fluorescent polarization method to evaluate the orientation of adsorbed molecules in uniaxial 2D layered materials. J Photochem Photobiol, A 181(1):44–49
138. López Arbeloa F, Martínez Martínez V (2006) Orientation of adsorbed dyes in the interlayer space of clays. 2 fluorescence polarization of rhodamine 6G in laponite films. Chem Mater 18 (6):1407–1416
139. Martinez V, Salleres S, Banuelos J, Arbeloa FL (2006) Application of fluorescence with polarized light to evaluate the orientation of dyes adsorbed in layered materials. J Fluoresc 16(2):233–240. doi:10.1007/s10895-005-0042-z
140. Bujdák J, Czímerová A, Arbeloa FL (2011) Two-step resonance energy transfer between dyes in layered silicate films. J Colloid Interface Sci 364(2):497–504. doi:10.1016/j.jcis.2011.08.042
141. Eguchi M, Tachibana H, Takagi S, Tryk DA, Inoue H (2007) Dichroic measurements on dicationic and tetracationic porphyrins on clay surfaces with visible-light-attenuated total reflectance. Bull Chem Soc Jpn 80:1350–1356. doi:10.1246/bcsj.80.1350
142. Yamaoka K, Sasai R, Takata N (2000) Electric linear dichroism. A powerful method for the ionic chromophore-colloid system as exemplified by dye and montmorillonite suspensions. Colloids Surf, A 175 (1–2):23-39
143. Inadomi T, Ikeda S, Okumura Y, Kikuchi H, Miyamoto N (2014) Photo-induced anomalous deformation of poly(N-Isopropylacrylamide) gel hybridized with an inorganic nanosheet liquid crystal aligned by electric field. Macromol Rapid Commun 35(20):1741–1746. doi:10.1002/marc.201400333
144. Egawa T, Watanabe H, Fujimura T, Ishida Y, Yamato M, Masui D, Shimada T, Tachibana H, Yoshida H, Inoue H, Takagi S (2011) Novel methodology to control the adsorption structure of cationic porphyrins on the clay surface using the “size-matching rule”. Langmuir 27(17):10722–10729. doi:10.1021/la202231k
145. Čeklovský A, Takagi S, Bujdák J (2011) Study of spectral behaviour and optical properties of cis/trans-bis (N-methylpyridinium-4-yl)diphenyl porphyrin adsorbed on layered silicates. J Colloid Interface Sci 360(1):26–30. doi:10.1016/j.jcis.2011.04.010
146. Čeklovský A, Czímerová A, Lang K, Bujdák J (2009) Effect of the layer charge on the interaction of porphyrin dyes in layered silicates dispersions. J Lumin 129(9):912–918. doi:10.1016/j.jlumin.2009.03.032
147. Čeklovský A, Czímerová A, Lang K, Bujdák J (2009) Layered silicate films with photochemically active porphyrin cations. Pure Appl Chem 81(8):1385–1396. doi:10.1351/pac-con-08-08-35
148. Hattori T, Tong ZW, Kasuga Y, Sugito Y, Yui T, Takagi K (2006) Hybridization of layered niobates with cationic dyes. Res Chem Intermed 32(7):653–669
149. Yui T, Kobayashi Y, Yamada Y, Tsuchino T, Yano K, Kajino T, Fukushima Y, Torimoto T, Inoue H, Takagi K (2006) Photochemical electron transfer though the interface of hybrid films of titania nano-sheets and mono-dispersed spherical mesoporous silica particles. Phys Chem Chem Phys 8(39):4585–4590. doi:10.1039/b609779k
150. Ishida Y, Shimada T, Masui D, Tachibana H, Inoue H, Takagi S (2011) Efficient excited energy transfer reaction in clay/porphyrin complex toward an artificial light-harvesting system. J Am Chem Soc 133(36):14280–14286. doi:10.1021/ja204425u
151. Bujdák J, Ratulovská J, Donauerová A, Bujdáková H (2016) Hybrid materials based on luminescent alkaloid berberine and saponite. J Nanosci Nanotechnol 16(8):7801–7804

152. Benard S, Leaustic A, Riviere E, Yu P, Clement R (2001) Interplay between magnetism and photochromism in spiropyran-$MnPS_3$ intercalation compounds. Chem Mater 13(10):3709–3716. doi:10.1021/cm011019j
153. Ogawa M, Yamamoto M, Kuroda K (2001) Intercalation of an amphiphilic azobenzene derivative into the interlayer space of a layered silicate, magadiite. Clay Miner 36(2):263–266
154. Ogawa M, Ishii T, Miyamoto N, Kuroda K (2003) Intercalation of a cationic azobenzene into montmorillonite. Appl Clay Sci 22(4):179–185. doi:10.1016/s0169-1317(02)00157-6
155. Bujdák J, Iyi N, Fujita T (2003) Isomerization of cationic azobenzene derivatives in dispersions and films of layered silicates. J Colloid Interface Sci 262(1):282–289. doi:10.1016/s0021-9797(03)00235-2
156. Umemoto T, Ohtani Y, Tsukamoto T, Shimada T, Takagi S (2014) Pinning effect for photoisomerization of a dicationic azobenzene derivative by anionic sites of the clay surface. Chem Commun 50(3):314–316. doi:10.1039/c3cc47353h
157. Ogawa M, Ishii T, Miyamoto N, Kuroda K (2001) Photocontrol of the basal spacing of azobenzene-magadiite intercalation compound. Adv Mater 13(14):1107–1109. doi:10.1002/1521-4095(200107)13:14<1107:AID-ADMA1107>3.0.CO;2-O
158. Ogawa M (2002) Photoisomerization of azobenzene in the interlayer space of magadiite. J Mater Chem 12(11):3304–3307. doi:10.1039/b204031j
159. Ishihara M, Hirase R, Mori M, Yoshioka H, Ueda Y (2009) Photoinduced spectral changes in hybrid thin films of functional dyes and inorganic layered material. Thin Solid Films 518 (2):857–860. doi:10.1016/j.tsf.2009.07.103
160. Gentili PL, Costantino U, Vivani R, Latterini L, Nocchetti M, Aloisi GG (2004) Preparation and characterization of zirconium phosphonate azobenzene intercalation compounds. A structural, photophysical and photochemical study. J Mater Chem 14 (10):1656–1662. doi:10.1039/b313828c
161. Okada T, Sakai H, Ogawa M (2008) The effect of the molecular structure of a cationic azo dye on the photoinduced intercalation of phenol in a montmorillonite. Appl Clay Sci 40(1–4):187–192. doi:10.1016/j.clay.2007.09.001
162. Okada T, Watanabe Y, Ogawa M (2005) Photoregulation of the intercalation behavior of phenol for azobenzene-clay intercalation compounds. J Mater Chem 15(9):987–992. doi:10.1039/b412707b
163. Boutton C, Kauranen M, Persoons A, Keung MP, Jacobs KY, Schoonheydt RA (1997) Enhanced second-order optical nonlinearity of dye molecules adsorbed onto Laponite particles. Clays Clay Miner 45(3):483–485
164. Ghofraniha N, Conti C, Ruocco G, Zamponi F (2009) Time-dependent nonlinear optical susceptibility of an out-of-equilibrium soft material. Phys Rev Lett 102 (3). doi:10.1103/PhysRevLett.102.038303
165. Ghofraniha N, Conti C, Ruocco G (2007) Aging of the nonlinear optical susceptibility in doped colloidal suspensions. Phys Rev B 75 (22). doi:10.1103/PhysRevB.75.224203
166. Laschewsky A, Wischerhoff E, Kauranen M, Persoons A (1997) Polyelectrolyte multilayer assemblies containing nonlinear optical dyes. Macromolecules 30(26):8304–8309
167. Suzuki Y, Tenma Y, Nishioka Y, Kamada K, Ohta K, Kawamata J (2011) Efficient two-photon absorption materials consisting of cationic dyes and clay minerals. J Phys Chem C 115(42):20653–20661. doi:10.1021/jp203809b
168. Suzuki Y, Tenma Y, Nishioka Y, Kawamata J (2012) Efficient nonlinear optical properties of dyes confined in interlayer nanospaces of clay minerals. Chem Asian J 7(6):1170–1179. doi:10.1002/asia.201200049
169. Suzuki Y, Sugihara H, Satomi K, Tominaga M, Mochida S, Kawamata J (2014) Two-photon absorption properties of an acetylene derivative confined in the interlayer space of a smectite. Appl Clay Sci 96:116–119. doi:10.1016/j.clay.2014.01.014
170. Epelde-Elezcano N, Duque-Redondo E, Martínez-Martínez V, Manzano H, López-Arbeloa I (2014) Preparation, photophysical characterization, and modeling of LDS722/Laponite 2D-Ordered hybrid films. Langmuir 30(33):10112–10117. doi:10.1021/la502081c

171. Coradin T, Clement R, Lacroix PG, Nakatani K (1996) From intercalation to aggregation: nonlinear optical properties of stilbazolium chromophores-MPS_3 layered hybrid materials. Chem Mater 8(8):2153–2158. doi:10.1021/cm960060x
172. Kawamata J, Suzuki Y, Tenma Y (2010) Fabrication of clay mineral-dye composites as nonlinear optical materials. Philos Mag 90(17–18):2519–2527. doi:10.1080/14786430903581304
173. Chakraborty S, Bhattacharjee D, Soda H, Tominaga M, Suzuki Y, Kawamata J, Hussain SA (2015) Temperature and concentration dependence of J-aggregate of a cyanine dye in a Laponite film fabricated by Langmuir-Blodgett technique. Appl Clay Sci 104:245–251. doi:10.1016/j.clay.2014.11.039
174. Kawamata J, Hasegawa S (2006) Clay-assisted disaggregation and stabilization in hemicyanine Langmuir-Blodgett films. J Nanosci Nanotechnol 6(6):1620–1624. doi:10.1166/jnn.2006.235
175. van Duffel B, Verbiest T, Van Elshocht S, Persoons A, De Schryver FC, Schoonheydt RA (2001) Fuzzy assembly and second harmonic generation of clay/polymer/dye monolayer films. Langmuir 17(4):1243–1249
176. Dudkina MM, Tenkovtsev AV, Pospiech D, Jehnichen D, Häußler L, Leuteritz A (2005) Nanocomposites of NLO chromophore-modified layered silicates and polypropylene. J Polym Sci, Part B: Polym Phys 43(18):2493–2502. doi:10.1002/polb.20532
177. Chao TY, Chang HL, Su WC, Wu JY, Jeng RJ (2008) Nonlinear optical polyimide/montmorillonite nanocomposites consisting of azobenzene dyes. Dyes Pigm 77(3):515–524. doi:10.1016/j.dyepig.2007.08.001
178. Yui T, Kameyama T, Sasaki T, Torimoto T, Takagi K (2007) Pyrene-to-porphyrin excited singlet energy transfer in LBL-deposited LDH nanosheets. J Porphyrins Phthalocyanines 11(5–6):428–433
179. Takagi S, Eguchi M, Shimada T, Hamatani S, Inoue H (2007) Energy transfer reaction of cationic porphyrin complexes on the clay surface: effect of sample preparation method. Res Chem Intermed 33(1–2):177–189
180. Bujdák J, Chorvát D, Iyi N (2010) Resonance energy transfer between rhodamine molecules adsorbed on layered silicate particles. J Phys Chem C 114(2):1246–1252. doi:10.1021/jp9098107
181. Ishida Y, Shimada T, Takagi S (2013) Artificial light-harvesting model in a self-assembly composed of cationic dyes and inorganic nanosheet. J Phys Chem C 117(18):9154–9163. doi:10.1021/jp4022757
182. Lu LD, Jones RM, McBranch D, Whitten D (2002) Surface-enhanced superquenching of cyanine dyes as J-aggregates on Laponite clay nanoparticles. Langmuir 18(20):7706–7713. doi:10.1021/la0259306
183. Eguchi M, Watanabe Y, Ohtani Y, Shimada T, Takagi S (2014) Switching of energy transfer reaction by the control of orientation factor between porphyrin derivatives on the clay surface. Tetrahedron Lett 55(16):2662–2666. doi:10.1016/j.tetlet.2014.03.027
184. Ras RHA, van Duffel B, Van der Auweraer M, De Schryver FC, Schoonheydt RA (2003) Molecular and particulate organisation in dye-clay films prepared by the Langmuir-Blodgett method. 2001—a Clay Odyssey:473–480
185. Hussain SA, Schoonheydt RA (2010) Langmuir-blodgett monolayers of cationic dyes in the presence and absence of clay mineral layers: N, N′-Dioctadecyl thiacyanine. Octadecyl Rhodamine B and Laponite Langmuir 26(14):11870–11877. doi:10.1021/la101078f
186. Hussain SA, Chakraborty S, Bhattacharjee D, Schoonheydt RA (2010) Fluorescence resonance energy transfer between organic dyes adsorbed onto nano-clay and langmuir-blodgett (LB) films. Spectrochim Acta A Mol Biomol Spectrosc 75(2):664–670. doi:10.1016/j.saa.2009.11.037
187. Dey D, Bhattacharjee D, Chakraborty S, Hussain SA (2013) Effect of nanoclay laponite and pH on the energy transfer between fluorescent dyes. J Photochem Photobiol, A 252:174–182

188. Olivero F, Carniato F, Bisio C, Marchese L (2014) Promotion of forster resonance energy transfer in a saponite clay containing luminescent polyhedral oligomeric silsesquioxane and rhodamine dye. Chem Asian J 9(1):158–165. doi:10.1002/asia.201300936
189. Dey D, Saha J, Roy AD, Bhattacharjee D, Hussain SA (2014) Development of an ion-sensor using fluorescence resonance energy transfer. Sens Actuators, B 195:382–388. doi:10.1016/j.snb.2014.01.065
190. Saha J, Datta Roy A, Dey D, Chakraborty S, Bhattacharjee D, Paul PK, Hussain SA (2015) Investigation of fluorescence resonance energy transfer between fluorescein and rhodamine 6G. Spectrochim Acta A Mol Biomol Spectrosc 149. doi:10.1016/j.saa.2015.04.027
191. Margulies L, Rozen H, Stern T, Rytwo G, Rubin B, Ruzo LO, Nir S, Cohen E (1993) Photostabilization of pesticides by clays and chromophores. Arch Insect Biochem Physiol 22 (3–4):467–486
192. Undabeytia T, Nir S, Tel-Or E, Rubin B (2000) Photostabilization of the herbicide norflurazon by using organoclays. J Agric Food Chem 48(10):4774–4779. doi:10.1021/jf9912405
193. Si YB, Zhou J, Chen HM, Zhou DM (2004) Photo stabilization of the herbicide bensulfuron-methyl by using organoclays. Chemosphere 54(7):943–950. doi:10.1016/j.chemosphere.2003.09.033
194. Kohno Y, Asai S, Shibata M, Fukuhara C, Maeda Y, Tomita Y, Kobayashi K (2014) Improved photostability of hydrophobic natural dye incorporated in organo-modified hydrotalcite. J Phys Chem Solids 75(8):945–950. doi:10.1016/j.jpcs.2014.04.010
195. Samuels M, Mor O, Rytwo G (2013) Metachromasy as an indicator of photostabilization of methylene blue adsorbed to clays and minerals. J Photochem Photobiol, B 121:23–26. doi:10.1016/j.jphotobiol.2013.02.004
196. Kohno Y, Totsuka K, Ikoma S, Yoda K, Shibata M, Matsushima R, Tomita Y, Maeda Y, Kobayashi K (2009) Photostability enhancement of anionic natural dye by intercalation into hydrotalcite. J Colloid Interface Sci 337(1):117–121. doi:10.1016/j.jcis.2009.04.065
197. Kohno Y, Kinoshita R, Ikoma S, Yoda K, Shibata M, Matsushima R, Tomita Y, Maeda Y, Kobayashi K (2009) Stabilization of natural anthocyanin by intercalation into montmorillonite. Appl Clay Sci 42(3–4):519–523. doi:10.1016/j.clay.2008.06.012
198. Ogawa M, Sohmiya M, Watase Y (2011) Stabilization of photosensitizing dyes by complexation with clay. Chem Commun 47(30):8602–8604. doi:10.1039/c1cc12392k
199. Shinozaki R, Nakato T (2008) Photochemical behavior of rhodamine 6G dye intercalated in photocatalytically active layered hexaniobate. Microporous Mesoporous Mater 113(1–3):81–89. doi:10.1016/j.micromeso.2007.11.005
200. Wang P, Cheng MM, Zhang ZH (2014) On different photodecomposition behaviors of rhodamine B on laponite and montmorillonite clay under visible light irradiation. J Saudi Chem Soc 18(4):308–316. doi:10.1016/j.jscs.2013.11.006
201. Raha S, Ivanov I, Quazi NH, Bhattacharya SN (2009) Photo-stability of rhodamine-B/montmorillonite nanopigments in polypropylene matrix. Appl Clay Sci 42 (3–4):661–666. doi:10.1016/j.clay.2008.06.008
202. Shinozaki R, Nakato T (2008) Photoelectrochemical behavior of a rhodamine dye intercalated in a photocatalytically active layered niobate and photochemically inert clay. J Ceram Soc Jpn 116(1352):555–560
203. Morimoto K, Tamura K, Iyi N, Ye JH, Yamada H (2011) Adsorption and photodegradation properties of anionic dyes by layered double hydroxides. J Phys Chem Solids 72(9):1037–1045. doi:10.1016/j.jpcs.2011.05.018
204. Caine MA, McCabe RW, Wang LC, Brown RG, Hepworth JD (2001) The influence of singlet oxygen in the fading of carbonless copy paper primary dyes on clays. Dyes Pigm 49 (3):135–143
205. Bujdák J, Jurečeková J, Bujdáková H, Lang K, Šeršeň F (2009) Clay mineral particles as efficient carriers of methylene blue used for antimicrobial treatment. Environ Sci Technol 43 (16):6202–6207. doi:10.1021/es900967g

206. Demel J, Kubat P, Jirka I, Kovar P, Pospisil M, Lang K (2010) Inorganic-organic hybrid materials: layered zinc hydroxide salts with intercalated porphyrin sensitizers. J Phys Chem C 114(39):16321–16328. doi:10.1021/jp106116n
207. Kafunkova E, Taviot-Gueho C, Bezdicka P, Klementova M, Kovar P, Kubat P, Mosinger J, Pospisil M, Lang K (2010) Porphyrins intercalated in Zn/Al and Mg/Al layered double hydroxides: properties and structural arrangement. Chem Mater 22(8):2481–2490. doi:10.1021/cm903125v
208. Jirickova M, Demel J, Kubat P, Hostomsky J, Kovanda F, Lang K (2011) Photoactive self-standing films made of layered double hydroxides with arranged porphyrin molecules. J Phys Chem C 115(44):21700–21706. doi:10.1021/jp207505n
209. Madhavan D, Pitchumani K (2002) Photoreactions in clay media: singlet oxygen oxidation of electron-rich substrates mediated by clay-bound dyes. J Photochem Photobiol, A 153(1–3):205–210
210. Bujdák J, Iyi N, Fujita T (2002) Aggregation and stability of 1,1′-diethyl-4,4′-cyanine dye on the surface of layered silicates with different charge densities. Colloids Surf A 207(1–3):207–214
211. Bujdák J, Iyi N, Fujita T (2003) Control of optical properties of adsorbed cyanine dyes via negative charge distribution on layered silicates. Solid State Chemistry V 90–91:463–468
212. Liu PF, Liu P, Zhao KC, Li L (2015) Photostability enhancement of azoic dyes adsorbed and intercalated into Mg-Al-layered double hydroxide. Opt Laser Technol 74:23–28
213. Kohno Y, Ito M, Kurata M, Ikoma S, Shibata M, Matsushima R, Tomita Y, Maeda Y, Kobayashi K (2011) Photo-induced coloration of 2-hydroxychalcone in the clay interlayer. J Photochem Photobiol, A 218(1):87–92. doi:10.1016/j.jphotochem.2010.12.007
214. Chakraborty S, Bhattacharjee D, Hussain SA (2014) Formation and control of excimer of a coumarin derivative in Langmuir-Blodgett films. J Lumin 145:824–831. doi:10.1016/j.jlumin.2013.09.001
215. Miyata H, Sugahara Y, Kuroda K, Kato C (1988) Synthesis of a viologen-tetratitanate intercalation. compound and its photochemical behaviour. J Chem Soc, Faraday Trans 84:2677–2682. doi:10.1039/f19888402677
216. Miyamoto N, Kuroda K, Ogawa M (2004) Visible light induced electron transfer and long-lived charge separated state in cyanine dye/layered titanate intercalation compounds. J Phys Chem B 108(14):4268–4274. doi:10.1021/jp035617s
217. Okada T, Matsutomo T, Ogawa M (2010) Nanospace engineering of methylviologen modified hectorite-like layered silicates with varied layer charge density for the adsorbents design. J Phys Chem C 114(1):539–545. doi:10.1021/jp9089886
218. Batista T, Chiorcea-Paquim AM, Brett AMO, Schmitt CC, Neumann MG (2011) Laponite RD/polystyrenesulfonate nanocomposites obtained by photopolymerization. Appl Clay Sci 53(1):27–32. doi:10.1016/j.clay.2011.04.007
219. Shiragami T, Mori Y, Matsumoto J, Takagi S, Inoue H, Yasuda M (2006) Non-aggregated adsorption of cationic metalloporphyrin dyes onto nano-clay sheets films. Colloids Surf A 284:284–289. doi:10.1016/j.colsurfa.2005.11.102
220. Kakegawa N, Ogawa M (2004) Effective luminescence quenching of tris(2,2-bipyridine) ruthenium(II) by methylviologen on clay by the aid of poly(vinylpyrrolidone). Langmuir 20(17):7004–7009. doi:10.1021/la036213u
221. de Souza GR, Fertonani FL, Pastre IA (2003) Espectroelectrochemical behavior of clay-dye structured systems. Ecletica Quim 28(1):77–83
222. Lazarin AM, Airoldi C (2008) Methylene blue intercalated into calcium phosphate—electrochemical properties and an ascorbic acid oxidation study. Solid State Sci 10(9):1139–1144. doi:10.1016/j.solidstatesciences.2007.11.023
223. Dilgin Y, Nisli G (2006) Flow injection photoamperometric investigation of ascorbic acid using methylene blue immobilized on titanium phosphate. Anal Lett 39(3):451–465. doi:10.1080/00003271050053605

224. Lazarin AM, Airoldi C (2004) Intercalation of methylene blue into barium phosphate-synthesis and electrochemical investigation. Anal Chim Acta 523(1):89–95. doi:10.1016/j.aca.2004.05.063
225. Sumitani M, Takagi S, Tanamura Y, Inoue H (2004) Oxygen indicator composed of an organic/inorganic hybrid compound of methylene blue, reductant, surfactant and saponite. Anal Sci 20(8):1153–1157
226. Shan D, Mousty C, Cosnier S, Mu SL (2003) A new Polyphenol oxidase biosensor mediated by azure B in laponite clay matrix. Electroanalysis 15(19):1506–1512. doi:10.1002/elan.200302740
227. Ishihara S, Iyi N, Labuta J, Deguchi K, Ohki S, Tansho M, Shimizu T, Yamauchi Y, Sahoo P, Naito M, Abe H, Hill JP, Ariga K (2013) Naked-eye discrimination of methanol from ethanol using composite film of oxoporphyrinogen and layered double hydroxide. ACS Appl Mater Interfaces 5(13):5927–5930. doi:10.1021/am401956s
228. Dey D, Bhattacharjee D, Chakraborty S, Hussain SA (2013) Development of hard water sensor using fluorescence resonance energy transfer. Sens Actuators, B 184:268–273. doi:10.1016/j.snb.2013.04.077
229. Esposito A, Raccurt O, Charmeau JY, Duchet-Rumeau J (2010) Functionalization of cloisite 30B with fluorescent dyes. Appl Clay Sci 50(4):525–532. doi:10.1016/j.clay.2010.10.007
230. Bur AJ, Roth SC, Start PR, Lee YH, Maupin PH (2007) Monitoring clay exfoliation during polymer/clay compounding using fluorescence spectroscopy. Trans Inst Measur Control 29 (5):403–416. doi:10.1177/0142331207073486
231. Banerjee S, Joshi M, Ghosh AK (2010) A spectroscopic approach for structural characterization of polypropylene/clay nanocomposite. Polym Compos 31(12):2007–2016. doi:10.1002/pc.20998
232. Gitis V, Dlugy C, Ziskind G, Sladkevich S, Lev O (2011) Fluorescent clays-similar transfer with sensitive detection. Chem Eng J 174(1):482–488. doi:10.1016/j.cej.2011.08.063
233. Marquez AES, Lerner DA, Fetter G, Bosch P, Tichit D, Palomares E (2014) Preparation of layered double hydroxide/chlorophyll a hybrid nano-antennae: a key step. Dalton Trans 43 (27):10521–10528. doi:10.1039/c4dt00113c
234. Teixeira-Neto ÃA, Izumi CMS, Temperini MLA, Ferreira AMDC, Constantino VRL (2012) Hybrid materials based on smectite clays and nutraceutical anthocyanins from the Açaí fruit. Eur J Inorg Chem 32:5411–5420. doi:10.1002/ejic.201200702
235. Choy JH, Kim YK, Son YH, Bin Choy Y, Oh JM, Jung H, Hwang SJ (2008) Nanohybrids of edible dyes intercalated in ZnAl layered double hydroxides. J Phys Chem Solids 69(5–6):1547–1551. doi:10.1016/j.jpcs.2007.11.009
236. Saelim NO, Magaraphan R, Sreethawong T (2011) Preparation of sol-gel TiO2/purified Na-bentonite composites and their photovoltaic application for natural dye-sensitized solar cells. Energy Convers Manage 52(8–9):2815–2818. doi:10.1016/j.enconman.2011.02.016
237. Kolesnikov MP, Kritsky MS (2001) Study of chemical structure and of photochemical activity of abiogenic flavin pigment. J Evol Biochem Physiol 37(5):507–514
238. Donauerová A, Bujdák J, Smolinská M, Bujdáková H (2015) Photophysical and antibacterial properties of complex systems based on smectite, a cationic surfactant and methylene blue. J Photochem Photobiol, B 151:135–141. doi:10.1016/j.jphotobiol.2015.07.018
239. Li DD, Miao CL, Wang XD, Yu XH, Yu JH, Xu RR (2013) AIE cation functionalized layered zirconium phosphate nanoplatelets: ion-exchange intercalation and cell imaging. Chem Commun 49(83):9549–9551. doi:10.1039/c3cc45041d
240. Kuo YM, Kuthati Y, Kankala RK, Wei PR, Weng CF, Liu CL, Sung PJ, Mou CY, Lee CH (2015) Layered double hydroxide nanoparticles to enhance organ-specific targeting and the anti-proliferative effect of cisplatin. J Mater Chem B 3(17):3447–3458. doi:10.1039/c4tb01989j
241. Rozen H, Margulies L (1991) Photostabilization of tetrahydro-2-(nitromethylene)-2H-1,3-thiazine adsorbed on clays. J Agric Food Chem 39(7):1320–1325
242. Banerjee K, Dureja P (1995) Photostabilization of quinalphos by crystal violet on the surface of kaolinite and palygorskite. Pestic Sci 43(4):333–337

243. Kievani MB, Edraki M (2015) Synthesis, characterization and assessment thermal properties of clay based nanopigments. Front Chem Sci Eng 9(1):40–45. doi:10.1007/s11705-015-1505-7
244. Beltran MI, Benavente V, Marchante V, Dema H, Marcilla A (2014) Characterisation of montmorillonites simultaneously modified with an organic dye and an ammonium salt at different dye/salt ratios. Properties of these modified montmorillonites EVA nanocomposites. Appl Clay Sci 97–98:43–52. doi:10.1016/j.clay.2014.06.001
245. Marchante V, Benavente V, Marcilla A, Martinez-Verdu FM, Beltran MI (2013) Ethylene vinyl acetate/nanoclay-based pigment composites: morphology, rheology, and mechanical, thermal, and colorimetric properties. J Appl Polym Sci 130(4):2987–2994. doi:10.1002/app.39422
246. Marchante V, Marcilla A, Benavente V, Martinez-Verdu FM, Beltran MI (2013) Linear low-density polyethylene colored with a nanoclay-based pigment: morphology and mechanical, thermal, and colorimetric properties. J Appl Polym Sci 129(5):2716–2726. doi:10.1002/app.38903
247. Aloisi GG, Costantino U, Latterini L, Nocchetti M, Camino G, Frache A (2006) Preparation and spectroscopic characterisation of intercalation products of clay and of clay-polypropylene composites with rhodamine B. J Phys Chem Solids 67(5–6):909–914. doi:10.1016/j.jpcs.2006.01.003
248. Smitha VS, Manjumol KA, Ghosh S, Brahmakumar M, Pavithran C, Perumal P, Warrier KG (2011) Rhodamine 6G intercalated montmorillonite nanopigments-polyethylene composites: facile synthesis and ultravioletstability study. J Am Ceram Soc 94(6):1731–1736. doi:10.1111/j.1551-2916.2010.04326.x
249. Zimmermann A, Jaerger S, Zawadzki SF, Wypych F (2013) Synthetic zinc layered hydroxide salts intercalated with anionic azo dyes as fillers into high-density polyethylene composites: first insights. J Polym Res 20(9). doi:10.1007/s10965-013-0224-3
250. da Silva MLN, Marangoni R, da Silva AH, Wypych F, Schreiner WH (2013) Poly(vinyl alcohol) composites containing layered hydroxide salts, intercalated with anionic azo dyes (Tropaeolin 0 and Tropaeolin 0). Polimeros 23(2):248–256. doi:10.1590/s0104-14282013005000026
251. Marangoni R, Gardolinski J, Mikowski A, Wypych F (2011) PVA nanocomposites reinforced with Zn2Al LDHs, intercalated with orange dyes. J Solid State Electrochem 15 (2):303–311. doi:10.1007/s10008-010-1056-2
252. Giovanella U, Leone G, Galeotti F, Mroz W, Meinardi F, Botta C (2014) FRET-assisted deep-blue electroluminescence in intercalated polymer hybrids. Chem Mater 26(15):4572–4578. doi:10.1021/cm501870e
253. Rafiemanzelat F, Adli V, Mallakpour S (2015) Effective preparation of clay/waterborne Azo-containing polyurethane nanocomposite dispersions incorporated anionic groups in the chain termini. Des Monomers Polym 18(4):303–314. doi:10.1080/15685551.2014.999459
254. Monteiro A, Jarrais B, Rocha IM, Pereira C, Pereira MFR, Freire C (2014) Efficient immobilization of montmorillonite onto cotton textiles through their functionalization with organosilanes. Appl Clay Sci 101:304–314. doi:10.1016/j.clay.2014.08.019
255. Zavodchikova AA, Safonov VV, Solina EV, Ivanov VB (2014) Ultraviolet paints based on nanopigments for printing on textile materials. Text Res J 84(13):1400–1410. doi:10.1177/0040517514523177
256. Ito K, Kuwabara M, Fukunishi K, Fujiwara Y (1997) Thermal recording media using clay-fluoran dye intercalation as a stable colour former. Dyes Pigm 34(4):297–306
257. Ito K, Zhou N, Fukunishi K, Fujiwara Y (1994) Potential use of clay-cationic dye complex for dye fixation in thermal dye-transfer printing. J Imaging Sci Technol 38(6):575–579
258. Ito K, Kuwabara M, Fukunishi K, Fujiwara Y (1996) Application of clay-cationic dye intercalation to image fixation in thermal dye transfer printing. J Imaging Sci Technol 40(3):275–280
259. Takashima M, Sano S, Ohara S (1993) Improved fastness of carbonless paper color images with a new trimethine leuco dye. J Imaging Sci Technol 37(2):163–166

260. Ito K, Fukunishi K (1997) Alternate intercalation of fluoran dye and tetra-n-decylammonium ion induced by electrolysis in acetone-clay suspension. Chem Lett 4:357–358
261. Hassanien MM, Abou-El-Sherbini KS, Al-Muaikel NS (2010) Immobilization of methylene blue onto bentonite and its application in the extraction of mercury (II). J Hazard Mater 178(1–3):94–100. doi:10.1016/j.jhazmat.2010.01.048